
Meta-Model-Based Meta-Policy Optimization

Takuya Hiraoka^{1,2,3}, Takahisa Imagawa², Voot Tangkaratt³, Takayuki Osa^{3,4},
Takashi Onishi^{1,2}, and Yoshimasa Tsuruoka^{2,5}

¹NEC Corporation

²National Institute of Advanced Industrial Science and Technology

³RIKEN Center for Advanced Intelligence Project

⁴Kyushu Institute of Technology

⁵The University of Tokyo

{takuya-h1, takashi.onishi}@nec.com

osa@brain.kyutech.ac.jp, voot.tangkaratt@riken.jp

imagawa.t@aist.go.jp, tsuruoka@logos.t.u-tokyo.ac.jp

Abstract

Model-based reinforcement learning (MBRL) has been applied to meta-learning settings and demonstrated its high sample efficiency. However, in previous MBRL for meta-learning settings, policies are optimized via rollouts that fully rely on a predictive model for an environment, and thus its performance in a real environment tends to degrade when the predictive model is inaccurate. In this paper, we prove that the performance degradation can be suppressed by using branched meta-rollouts. Based on this theoretical analysis, we propose meta-model-based meta-policy optimization (M3PO), in which the branched meta-rollouts are used for policy optimization. We demonstrate that M3PO outperforms existing meta reinforcement learning methods in continuous-control benchmarks.

1 Introduction

Reinforcement learning (RL) methods have achieved remarkable successes in many decision-making tasks, such as playing video games or controlling robots (e.g., [9, 20]). In conventional RL methods, when multiple tasks are to be solved, a policy of each task is independently learned with millions of training samples from the environment for individual tasks. This independent learning with a large number of samples prevents the conventional RL methods from being applied to the practical problems that require a variety of policies to solve multiple tasks (e.g., robotic manipulation problems involving grasping or moving different types of objects [39]). Meta-learning methods [29, 35] have recently gained much attention as a solution to this problem; they learn a structure shared in the tasks by using a large number of samples collected across the parts of the tasks. Once learned, these methods can adapt quickly to new (the rest of) tasks with a small number of samples given in them.

In previous work, meta RL methods have been introduced into both model-free and model-based settings. For model-free settings, there are two main types of approaches proposed so far: recurrent-based policy adaptation [4, 19, 26, 37] and gradient-based policy adaptation [1, 6, 7, 10, 27, 31]. In these approaches, policies adapt to a new task by leveraging the history of past trajectories; following previous work [3], we refer to these adaptive policies as **meta-policies** in our paper. These model-free RL methods with meta-learning require more training samples than conventional RL because, in addition to learning control policies, learning of policy adaptation is also required [18].

For model-based settings, Sæmundsson et al. [28] use a predictive model (also known as a transition model) based on a latent variable Gaussian process for model predictive control. Nagabandi et

al. [22, 23] introduced both recurrent-based and gradient-based meta-learning methods into model-based RL. In these works, the predictive models adapt to a new task by leveraging the history of past trajectories; in analogy to the meta-policy, we refer to these adaptive predictive models as **meta-models** in our paper. In general, these meta-model-based RL approaches are more sample efficient than the model-free approaches because they leverage more supervision. However, in previous meta-model-based RL, the meta-policy (or the course of future actions) is optimized via rollouts relying fully on the meta-model, and thus its performance in a real environment tends to degrade when the meta-model is inaccurate.

In this paper, we address this problem in meta-model-based RL. At first, as preliminaries, we review the related work (Section 2) and partially observable Markov decision processes (POMDPs) (Section 3). Next, we formulate meta-model-based RL as solving a POMDP (Section 4) and then conduct theoretical analysis on its performance guarantee (Section 5). Our analysis results show that, if the meta-model is used in the branched rollout manner [15], the performance degradation due to the meta-model inaccuracy can be significantly suppressed compared to the full meta-model-based rollouts case. Based on this analysis result, we propose a practical meta-model-based RL method called Meta-Model-based Meta-Policy Optimization (M3PO), in which the meta-model is used in the branched rollout manner (Section 6). Finally, we experimentally demonstrate that M3PO outperforms existing methods in continuous-control benchmarks (Section 7). Our main contribution are as follows: (1) providing performance guarantees of meta-model-based RL (Theorem 1, Theorem 2, and Theorem 3), and (2) proposing and showing the effectiveness of M3PO.

2 Related work

In this section, we review related work on POMDPs and theoretical analysis in model-based RL.

Partially observable Markov decision processes¹: In our paper, we formulate model-based RL in a meta-learning setting as solving a POMDP, and provide its performance guarantee under the branched rollout setting. POMDPs are a long-studied problem (e.g., [8, 32, 33]) and there are many works that discuss a performance guarantee of RL methods for solving POMDPs. However, to the best of our knowledge, the performance guarantee of the RL methods based on branched rollouts has not been discussed in the literature. On the other hand, some researchers [14, 16, 40] propose model-free RL methods for solving a POMDP without prior knowledge of the accurate model. However, they do not provide theoretical analyses of performance. In this work, by contrast, we propose a model-based RL method, and provide theoretical analyses on its performance guarantee.

Theoretical analysis on the performance of model-based RL: There are previous works in which theoretical analysis on the performance of model-based RL is provided [5, 12, 15, 17, 25]. In these theoretical analyses, standard Markov decision processes (MDPs) are assumed, and the meta-learning (or POMDP) setting is not discussed. In contrast, our work provides a theoretical analysis on the meta-learning (and POMDP) setting, substantially extending Janner et al’s work [15]. They analyze the performance guarantee of branched rollouts with a predictive model on MDPs, and introduce branched rollouts into a model-based RL algorithm. We extend their analysis and algorithm to a meta learning (POMDP) case. In addition, as a part of our analysis, we make a modification to their theorems of the branched rollouts so that some important premises (e.g., the effect of multiple model-based rollout factors) are more properly reflected into the theorems. See A.1 in the appendix for more detailed discussion about our contribution.

3 Partially observable Markov decision processes

We formalize our problem with a POMDP, which is defined as the tuple $\langle \mathcal{O}, \mathcal{S}, \mathcal{A}, p_{\text{ob}}, r, \gamma, p_{\text{st}} \rangle$. Here, \mathcal{O} is the set of observations, \mathcal{S} is the set of hidden states, \mathcal{A} is the set of actions, $p_{\text{ob}} := \mathcal{O} \times \mathcal{S} \times \mathcal{A} \rightarrow (0, 1)$ is the observation probability, $p_{\text{st}} := \mathcal{S} \times \mathcal{S} \times \mathcal{A} \rightarrow (0, 1)$ is the state transition probability, $r : \mathcal{S} \times \mathcal{A} \rightarrow \mathbb{R}$ is a reward function, and $\gamma \in [0, 1)$ is a discount factor. At time step t , these functions are used as $p_{\text{st}}(s_t | s_{t-1}, a_{t-1})$, $p_{\text{ob}}(o_t | s_t, a_{t-1})$ ², and $r_t = r(s_t, a_t)$. The agent cannot directly observe the hidden state, but receives the observation instead. The agent

¹We include works on Bayes-adaptive MDPs [8, 40] as works on POMDPs because they are a special case of POMDPs.

²For simplicity, we use these probabilities by abbreviating the subscripts “st” and “ob.”

Algorithm 1 Abstract Meta Model-based Meta-Policy Optimization (Abstract M3PO)

- 1: Initialize meta-policy π_ϕ , meta-model p_θ , and dataset \mathcal{D} .
 - 2: **for** N epochs **do**
 - 3: Collect trajectories from environment according to π_ϕ : $\mathcal{D} = \mathcal{D} \cup \{(h_t, o_{t+1}, r_t)\}$.
 - 4: Optimize π_ϕ and p_θ : $(\phi, \theta) \leftarrow \arg \max_{(\phi, \theta)} \mathbb{E}_{a \sim \pi_\phi, h \sim p_\theta} [R] - C(\epsilon_m(\theta), \epsilon_\pi(\phi))$.
 - 5: **end for**
-

selects an action based on a policy $\pi := p(a_{t+1}|h_t)$, where h_t is a history (the past trajectories), i.e., $h_t := \{a_0, o_0, \dots, a_t, o_t\}$. We denote the set of the histories by \mathcal{H} . Given the definition of the history, the history transition probability can be defined as $p(h_{t+1}|a_{t+1}, h_t) := p(o_{t+1}|h_t)$. Here, $p(o_{t+1}|h_t) := \sum_{s_{t+1}} \sum_{s_t} p(s_t|h_t)p(s_{t+1}|s_t, a_t)p(o_{t+1}|s_{t+1}, a_t)$ where $p(s_t|h_t)$ is the belief about the hidden state. The goal of reinforcement learning in the POMDP is to find the optimal policy π^* that maximizes the expected return $R := \sum_{t=0}^{\infty} \gamma^t r_t$ (i.e., $\pi^* = \arg \max_{\pi} \mathbb{E}_{a \sim \pi, h \sim p} [R]$).

4 Formulating model-based RL in meta-learning settings

In this section, we formulate model-based RL in the meta-learning setting as solving a POMDP by using a parameterized meta-policy and meta-model. As with [22, 23], we assume online adaptation situations where the agent can leverage a small number of samples to adapt quickly to a new task. Here, a task specifies the transition probability and the reward function. The task information cannot be observed by the agent, and may change at each step in an episode (i.e., the task information is included in the hidden state s). In the previous meta-learning literature (e.g., [7, 22, 23, 26]), the policy and the predictive model adapt to a new task by using past trajectories in an episode. As we noted earlier, we call this sort of adaptive policy and predictive model a meta-policy and a meta-model, respectively.

We define a meta-policy and a meta-model as $\pi_\phi(a_{t+1}|h_t)$ and $p_\theta(r_t, o_{t+1}|h_t)$, respectively. Here, ϕ and θ are learnable parameters for the meta-policy and the meta-models. r_{t+1} and s_{t+1} are assumed to be conditionally independent given h_t , i.e., $p_\theta(r_t, o_{t+1}|h_t) = p_\theta(r_t|h_t) \cdot p_\theta(o_{t+1}|h_t)$. As with $p(h_{t+1}|a_{t+1}, h_t)$, we define the meta-model for the history as $p_\theta(h_{t+1}|a_{t+1}, h_t) := p_\theta(o_{t+1}|h_t)$.

We use the parameterized meta-model and the meta-policy as in Algorithm 1. In this algorithm, the following procedures are repeated: 1) sample collection from the real environment with the meta-policy and store them into a dataset \mathcal{D} , 2) optimization of the meta-policy and the meta-model to maximize $\mathbb{E}_{a \sim \pi_\phi, h \sim p_\theta} [R] - C(\epsilon_m(\theta), \epsilon_\pi(\phi))$. Here, $\mathbb{E}_{a \sim \pi_\phi, h \sim p_\theta} [R]$ is a meta-model return, i.e., the return of the meta-policy on the meta-model (for simplicity, we use the abbreviated style $\mathbb{E}_{\pi_\phi, p_\theta} [R]$), and $C(\epsilon_m(\theta), \epsilon_\pi(\phi))$ is a discrepancy depending on the two error quantities ϵ_m and ϵ_π (their detailed definitions are introduced in the next section). In the next section, we conduct theoretical analyses for the performance guarantee of Algorithm 1.

Supplement: Some readers may be concerned that “in a typical meta-RL setting, the objective to be optimized is usually defined as the expected return with respect to the task distribution, but such an objective is not included in the formulation in Section 4.” In A.4 in the appendix, we show that such an objective can actually be derived from $\mathbb{E}_{a \sim \pi_\phi, h \sim p_\theta} [R]$ by specializing our formulation (i.e., our formulation covers the typical meta-RL setting). Nevertheless, in this paper, we avoid such specialization in order to provide analysis and algorithms covering a wider range of meta-RL settings.

5 Performance guarantees of meta-model-based RL

In this section, we analyze the performance guarantee of meta-model-based RL with an inaccurate meta-model. In Section 5.1, we provide the performance guarantee in a full meta-model-based rollout case (Theorem 1) as a baseline to be improved. In Section 5.2, we introduce the notion of branched meta-rollout and show that, under the one-step branched meta-rollout, performance degradation due to meta-model error can be suppressed compared to the full meta-model-rollout case (Theorem 2). In Section 5.3, we show that, by considering 1) meta-model error under the current

meta-policy and 2) appropriately adjusted length for the branched meta-rollout, the performance degradation can be further suppressed (Theorem 3). These analysis results indicate that the branched meta-rollout with appropriate rollout length is better way of using the model for suppressing the performance degradation due to the meta-model error than the full model rollout.

5.1 Performance guarantee in a full meta-model-based rollout case

Our goal is to outline a theoretical framework in which we can provide performance guarantees for Algorithm 1. To show the guarantees, we construct a lower bound taking the following form: $\mathbb{E}_{\pi_{\phi}, p}[R] \geq \mathbb{E}_{\pi_{\phi}, p_{\theta}}[R] - C(\epsilon_m(\theta), \epsilon_{\pi}(\phi))$, where $\mathbb{E}_{\pi_{\phi}, p}[R]$ denotes a true return, i.e., the return of the meta-policy in the true environment. The discrepancy between these returns, C , which determines the amount of performance degradation, can be expressed as the function of two error quantities of the meta-model: generalization error due to sampling, and distribution shift due to the updated meta-policy. For our analysis, we define the bounds of the generalization error ϵ_m and the distribution shift ϵ_{π} as follows:

Definition 1. $\epsilon_m(\theta) := \max_t \mathbb{E}_{a \sim \pi_{\mathcal{D}}, h \sim p}[D_{TV}(p(h_{t+1}|a_{t+1}, h_t)||p_{\theta}(h_{t+1}|a_{t+1}, h_t))]$, where D_{TV} is a total variation distance and $\pi_{\mathcal{D}}$ is the data collection policy that actions contained in \mathcal{D} follow³.

Definition 2. $\epsilon_{\pi}(\phi) := \max_{h_t} D_{TV}(\pi_{\mathcal{D}}(a_{t+1}|h_t)||\pi_{\phi}(a_{t+1}|h_t))$.

In addition to these error bounds, we assume that we can know the bound of the reward expected on the basis of a belief; $r_{max} > |\sum_{s_t} p(s_t|h_t)r(s_t, a_t)|$.

Now we present our bound, which is an extension of the theorem proposed in [15] to our setting.

Theorem 1 (The POMDP extension of Theorem 4.1. in [15]). *Let the expected TV-distance between two history transition distributions be bounded at each timestep by ϵ_m and the meta-policy divergence be bounded by ϵ_{π} . Then the true returns is bounded from below by meta-model returns of the meta-policy and discrepancy:*

$$\mathbb{E}_{\pi_{\phi}, p}[R] \geq \mathbb{E}_{\pi_{\phi}, p_{\theta}}[R] - \underbrace{r_{max} \left[\frac{2\gamma(\epsilon_m + 2\epsilon_{\pi})}{(1-\gamma)^2} + \frac{4\epsilon_{\pi}}{(1-\gamma)} \right]}_{C(\epsilon_m(\theta), \epsilon_{\pi}(\phi))} \quad (1)$$

This theorem implies that the discrepancy of the returns under full meta-model rollout scales linearly with both ϵ_m and ϵ_{π} . If we can reduce the discrepancy, the two returns are closer to each other and thus the performance degradation is more significantly suppressed. In the next section, we discuss a new meta-model usage to reduce the discrepancy induced by the meta-model error (i.e., ϵ_m).

5.2 Performance guarantee in the branched meta-rollout case

The analysis of Theorem 1 relies on running full rollouts through the meta-model, allowing meta-model errors to compound. This is reflected in the bound by a factor scaling quadratically with the effective horizon, $1/(1-\gamma)$. In such cases, we can improve the algorithm by choosing to rely less on the meta-model and instead more on real data collected from the true environment when the meta-model is inaccurate.

In order to allow for dynamic adjustment between meta-model-based and model-free rollouts, we introduce the notion of a **branched meta-rollout**⁴, in which we begin a rollout from a history under the previous meta-policy's history distribution $p_{\pi_{\mathcal{D}}}(h_t)$ and run k steps according to π_{ϕ} under the learned meta-model p_{θ} . Under such a scheme, the true return can be bounded from below as follows:

Theorem 2. *Under the k -branched meta-rollout, using the bound of a meta-model error under $\pi_{\mathcal{D}}$, $\epsilon_m = \max_t \mathbb{E}_{a \sim \pi_{\mathcal{D}}, h \sim p, t}[D_{TV}(p(h'|h, a)||p_{\theta}(h'|h, a))]$, the bound of the meta-policy shift $\epsilon_{\pi} = \max_{h_t} D_{TV}(\pi_{\mathcal{D}}||\pi_{\phi})$, and the return on the meta-model $\mathbb{E}_{(a, h) \sim \mathcal{D}_{model}}[R]$ where \mathcal{D}_{model} is the set*

³As with [15], to simplify our analysis, we assume that the meta-model can accurately estimate reward. We discuss the case in which the reward prediction of a meta-model is inaccurate in A.6 in the appendix.

⁴This can be seen as the extension of a "branched rollout" proposed in [15, 34] to meta-learning settings.

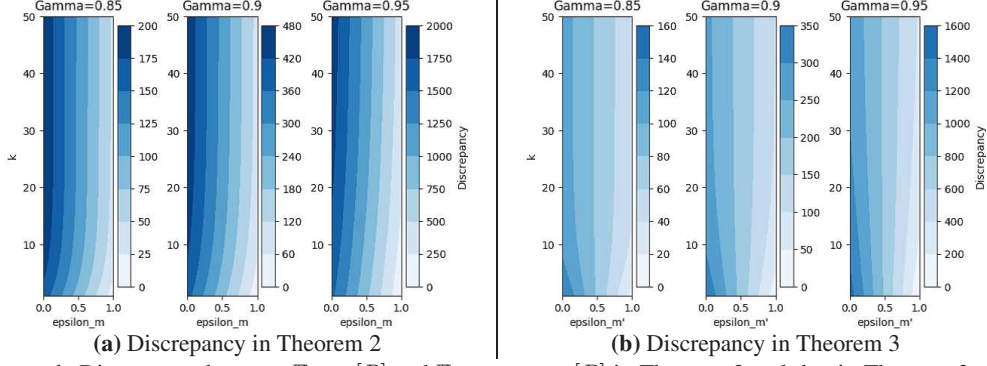


Figure 1: Discrepancy between $\mathbb{E}_{\pi_{\phi,p}}[R]$ and $\mathbb{E}_{(a,h) \sim \mathcal{D}_{\text{model}}}[R]$ in Theorem 2 and that in Theorem 3. Each vertical axis represents $k \in [1, 50]$ and each horizontal axis represents $\epsilon_m, \epsilon_{m'} \in [0, 1]$. In all figures, for evaluating the discrepancy values, we set the other variables as $r_{\max} = 1$, $\epsilon_{\pi} = 1 - \epsilon_m$ for (a), and $\epsilon_{\pi} = 1 - \epsilon_{m'}$ for (b).

of samples collected through branched rollouts, the following inequation holds,

$$\mathbb{E}_{\pi_{\phi,p}}[R] \geq \mathbb{E}_{(a,h) \sim \mathcal{D}_{\text{model}}}[R] - r_{\max} \left\{ \frac{1 + \gamma^2}{(1 - \gamma)^2} 2\epsilon_{\pi} + \frac{\gamma - k\gamma^k + (k-1)\gamma^{k+1}}{(1 - \gamma)^2} (\epsilon_{\pi} + \epsilon_m) \right. \\ \left. + \frac{\gamma^k - \gamma}{\gamma - 1} (\epsilon_{\pi} + \epsilon_m) + \frac{\gamma^k}{1 - \gamma} (k+1)(\epsilon_{\pi} + \epsilon_m) \right\}. \quad (2)$$

The discrepancy factors relying on ϵ_m at $k = 1$ in Theorem 2 are smaller than the discrepancy factors relying on ϵ_m in Theorem 1 (see Corollary 1 in the appendix). This indicates that the performance degradation due to the meta-model error can be more suppressed than that under the full meta-based-model rollout.

5.3 Meta-model generalization in practice

Figure 1a shows that the discrepancy value in Theorem 2 tends to monotonically increase as the value of k increases, regardless of the values of γ and ϵ_m ; this means that the optimal value of k is always 1. However, intuitively, we may expect that there is an optimal value for k that is higher than 1 when the meta-model error is small; as will be shown in this section, this intuition is correct. One of the main reasons for the mismatch of the intuition and the tendency of the discrepancy in Theorem 2 is that, for its analysis, the meta-model error on the data collection meta-policy $\pi_{\mathcal{D}}$ (i.e., ϵ_{π}) is used instead of that on the current meta-policy π_{ϕ} . This ignorance of the meta-model error on the current meta-policy induces the pessimistic estimation of the discrepancy in the analysis (see the evaluation of “term B” and “term C” in the proof of Theorem 4 via the proof of Theorem 2 in the appendix for more details).

To estimate the discrepancy more tightly, as in [15], we introduce the assumption that the meta-model error on the current meta-policy can be approximated by ϵ_{π} and ϵ_m :

Assumption 1. An approximated meta-model error on a current policy $\epsilon_{m'}: \epsilon_{m'}(\epsilon_{\pi}) \approx \epsilon_m + \epsilon_{\pi} \frac{d\epsilon_{m'}}{d\epsilon_{\pi}}$, where $\frac{d\epsilon_{m'}}{d\epsilon_{\pi}}$ is the local change of $\epsilon_{m'}$ with respect to ϵ_{π}

To see the tendency of this approximated meta-model error, we plot the empirical value of $d\epsilon_{m'}/d\epsilon_{\pi}$, varying the size of training samples for the meta-model in Figure 7 in A.10. The figure shows that, as the training sample size increases, the value tends to gradually approach zero. This means that training meta-models with more samples provide better generalization on the nearby distributions.

Equipped with the approximated meta-model’s error on the distribution of the current meta-policy π_{ϕ} , we arrive at the following bound:

Algorithm 2 Meta-Model-based Meta-Policy Optimization with Deep RL (M3PO)

```
1: Initialize meta-policy  $\pi_\phi$ , meta-model  $p_\theta$ , environment dataset  $\mathcal{D}_{\text{env}}$ , meta-model dataset  $\mathcal{D}_{\text{model}}$ .
2: for  $N$  epochs do
3:   Train meta-model  $p_\theta$  with  $\mathcal{D}_{\text{env}}$ :  $\theta \leftarrow \arg \max_{\theta} \mathbb{E}_{\mathcal{D}_{\text{env}}} [p_\theta(r_t, o_{t+1}|h_t)]$ 
4:   for  $E$  steps do
5:     Take actions according to  $\pi_\phi$ ; add the trajectory to  $\mathcal{D}_{\text{env}}$ 
6:     for  $M$  model rollouts do
7:       Sample  $h_t$  uniformly from  $\mathcal{D}_{\text{env}}$ 
8:       Perform  $k$ -step meta-model rollout starting from  $h_t$  using meta-policy  $\pi_\phi$ ; add fictitious
       trajectories to  $\mathcal{D}_{\text{model}}$ 
9:     end for
10:    for  $G$  gradient updates do
11:      Update policy parameters with  $\mathcal{D}_{\text{model}}$ :  $\phi \leftarrow \phi - \nabla_{\phi} J_{\mathcal{D}_{\text{model}}}(\phi)$ 
12:    end for
13:  end for
14: end for
```

Theorem 3. Let $\epsilon_{m'} \geq \max_t \mathbb{E}_{a \sim \pi_\phi, h \sim p} [D_{TV}(p(h'|h, a) || p_\theta(h'|h, a))]$,

$$\mathbb{E}_{\pi_\phi, p} [R] \geq \mathbb{E}_{(a, h) \sim \mathcal{D}_{\text{model}}} [R] - r_{\max} \left\{ \frac{1 + \gamma^2}{(1 - \gamma)^2} 2\epsilon_\pi + \frac{\gamma - k\gamma^k + (k - 1)\gamma^{k+1}}{(1 - \gamma)^2} (\epsilon_{m'} - \epsilon_\pi) \right. \\ \left. + \frac{\gamma^k - \gamma}{\gamma - 1} (\epsilon_{m'} - \epsilon_\pi) + \frac{\gamma^k}{1 - \gamma} (k + 1) (\epsilon_{m'} - \epsilon_\pi) \right\}. \quad (3)$$

Given that $\epsilon_m = \epsilon_{m'}$, it is obvious that the discrepancy in Theorem 3 is equal to or smaller than that in Theorem 2. In the discrepancy in Theorem 3, all terms except the first term become negative when $\epsilon_{m'} < \epsilon_\pi$ ⁵. This implies that the optimal k that minimizes the discrepancy can take on the value higher than 1 when the meta-model error is relatively small. The empirical trend of the discrepancy value (Figure 1b) supports it; when $\epsilon_{m'}$ is lower than 0.5 (i.e., $\epsilon_{m'} < \epsilon_\pi$), the discrepancy values decrease as the value of k grows regardless of the value of γ . This result motivates us to set k to the value higher than 1 in accordance with the meta-model error for reducing the discrepancy.

To recap our analysis, the use of branched meta-rollouts with appropriate rollout lengths (i.e., the value of k) contribute to reducing the returns' discrepancy relying on the meta-model error and thus lead to suppressing the performance degradation due to the meta-model inaccuracy.

6 Meta-model-based meta-policy optimization with deep RL

In the previous section, we show that the use of branched meta-rollouts with appropriate rollout lengths can suppress the performance degradation induced by the meta-model inaccuracy. In this section, based on this result, we propose to modify Algorithm 1 so that the meta-policy and the meta-model are optimized on the basis of the lower bound of true return with the branched meta-rollouts, $\mathbb{E}_{(a, h) \sim \mathcal{D}_{\text{model}}} [R] - C(\epsilon_m(\theta), \epsilon_\pi(\phi))$, instead of $\mathbb{E}_{\pi, p} [R] - C(\epsilon_m(\theta), \epsilon_\pi(\phi))$.

More specifically, we propose the following modifications to Algorithm 1:

Meta-policy optimization: The meta-policy is optimized with branched meta-rollouts $\mathbb{E}_{(a, h) \sim \mathcal{D}_{\text{model}}} [R]$ ⁶. For the optimization, we adapt PEARL [26] because it achieved good learning performance in meta-learning settings [26]. To adapt PEARL, we use the imagination trajectories generated from the branched meta-rollouts for optimizing the meta-policy (and value functions) instead of real trajectories. Formally, π_ϕ is optimized by using the gradient of optimization

⁵Such situations may arise when the meta-model is learnt with a large amount of data and $\frac{d\epsilon_{m'}}{d\epsilon_\pi}$ is nearly zero (recall the result in Figure 7), or environment dynamics over tasks are simple and easily approximated by the meta-model.

⁶To stabilize the learning, we omit $C(\epsilon_m(\theta), \epsilon_\pi(\phi))$ from the optimization objective for the meta-policy.

objective $J_{\mathcal{D}_{\text{model}}}(\phi) := \mathbb{E}_{(a,h) \sim \mathcal{D}_{\text{model}}} [D_{KL}(\pi_\phi || \exp(Q_{\pi_\phi} - V_{\pi_\phi}))]$, where $Q_{\pi_\phi}(a_{t+1}, h_t) := \mathbb{E}_{(r,h) \sim \mathcal{D}_{\text{model}}} [R|a_{t+1}, h_t]$ and $V_{\pi_\phi}(h_t) := \sum_{a_{t+1}} Q_{\pi_\phi}(a_{t+1}, h_t) \pi_\phi(a_{t+1}|h_t)$.

Meta-model optimization: The meta-model is optimized to minimize the discrepancy (i.e., ϵ_m). In practice, to simplify and stabilize learning, we learn the meta-model via maximum likelihood estimation⁷. For the meta-model, to reduce the model bias, we use a bootstrap ensemble of B dynamics models $\{p_\theta^1, \dots, p_\theta^B\}$. Here $p_\theta^i(r_t, o_{t+1}|h_t)$ is the i -th conditional Gaussian distribution with diagonal covariance: $p_\theta^i(r_t, o_{t+1}|h_t) = \mathcal{N}(r_{t+1}, o_{t+1} | \mu_\theta^i(h_t), \sigma_\theta^i(h_t))$, where μ_θ^i and σ_θ^i are the mean and the standard deviation, respectively. In our implementation, we use the recurrence-based architecture inspired by [23, 26]; at each evaluation of the model, $\{a_1, o_1, \dots, a_{t-1}, o_{t-1}\}$ in h_t is fed to a recurrent neural network, and then its hidden unit output and $\{a_t, o_t\}$ in h_t are fed to the feed-forward neural network that outputs the mean and standard deviation of the Gaussian distribution. We use the gated recurrent unit [2] for the recurrent neural network⁸.

The resulting algorithm is shown in Algorithm 2. The modifications ‘‘Meta-model optimization’’ and ‘‘Meta-policy optimization’’ in the last paragraph are reflected in line 3 and lines 4–13, respectively. In addition, as indicated by Theorem 2 and Theorem 3, appropriately setting k contributes to decreasing the discrepancy, and leads to the suppression of the performance degradation in the real environment. Thus, we treat k as a hyperparameter, and set it to different values for different environments so that the discrepancy decreases. For the experiments described in the next section, we set hyperparameters for this algorithm by grid search. A search result for the hyperparameter values is described in Table 1 in the appendix).

7 Experiments

In this section, we report our experiments⁹ aiming to answer the following questions: **Q.1:** Can our method (M3PO) outperforms existing meta-RL methods? **Q.2:** How do meta-model-rollout lengths affect the actual performance?

In our experiments, we compare our method (M3PO) with baseline methods; **PEARL** [26] and **Learning to adapt (L2A)** [22]. More detailed information is described in A.8 in the appendix. We conduct a comparative evaluation of the methods on a variety of simulated robot environments using the MuJoCo physics engine [36]. We prepare the environments proposed in the meta-RL [6, 22, 26, 27] and robust-RL [13, 24] literature: **Halfcheetah-fwd-bwd**, **Halfcheetah-pier**, **Ant-fwd-bwd**, **Ant-crippled-leg**, **Walker2D-randomparams**, and **Humanoid-direc**. In all the environments, the agent is required to adapt to a fluidly changing task that the agent cannot directly observe. Detailed information about each environment is described in A.9 in the appendix.

Regarding Q1, our experimental results indicate that M3PO outperforms existing meta RL methods. In Figure 2, the learning curves of M3PO and existing meta-RL methods (L2A and PEARL) on meta-training phases are shown, and they indicate that the sample efficiency of M3PO is better than L2A and PEARL¹⁰. L2A is trapped in poor performance (return) and it is not improved even when the training sample size increases, whereas M3PO avoids being trapped in such a poor performance. PEARL can improve meta-policy performance via training in all environments, but the degree of improvement of PEARL is smaller than that of M3PO. On the other hand, in some of the environments (e.g., Halfcheetah-pier), as the training sample size increases, the relative performance of M3PO against PEARL becomes worse. This indicates that, as with [21], dynamic switching from M3PO to PEARL or other model-free approaches needs to be considered to further improve overall performance.

Regarding Q2, we conducted an evaluation of M3PO by varying its model-rollout length k . The evaluation results (Figure 3) indicate that the performance is degraded when the model-rollout length is long (i.e., when the performance is significantly affected by the meta-model error). We can see

⁷The transition of ϵ_m over training epochs is shown in Figure 8 in the appendix, and it indicates that the model error tends to decrease as epochs elapse.

⁸We also tried to use the gradient-based MAML architecture [7] for our meta-models as with [23], but were unable to obtain reasonable results with it.

⁹The source code to replicate the experiments will be open to the public after the acceptance of this paper.

¹⁰Note that, in an early stage of the training phase, there are many test episodes in which unseen tasks appear. Therefore, the improvement of M3PO over L2A and PEARL at the early stage of learning indicates its high adaptation capability for unseen situations.

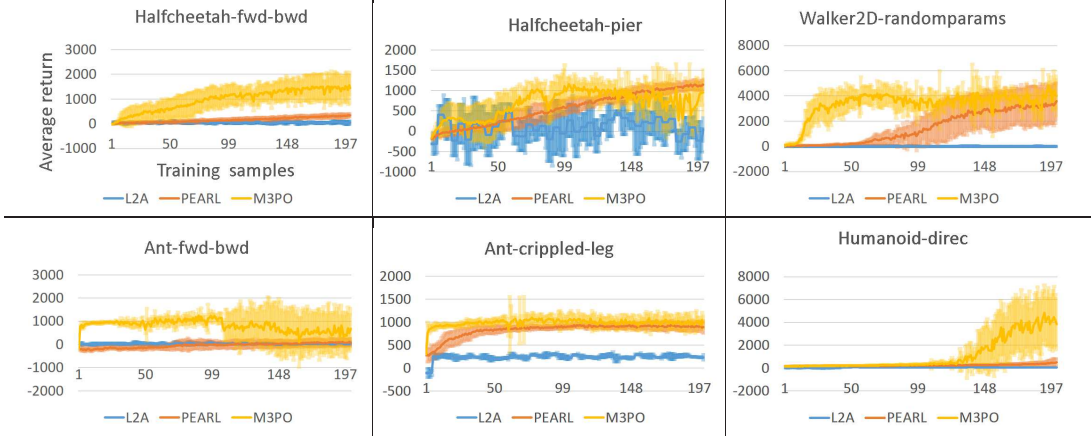


Figure 2: Learning curves. In each figure, the vertical axis represents returns, and the horizontal axis represents numbers of training samples (x1000). The meta-policy and meta-model are fixed and evaluated in terms of their expected returns on 50 episodes at every 5000 training samples for L2A and 1000 training samples for the other methods. In each episode, the task is initialized and changed randomly. Each method is evaluated at least in five trials, and the expected return on the 50 episodes is further averaged over the trials. The averaged expected returns and their standard deviations are plotted in the figures. We assigned an almost equal time budget for each method, and trials completed in the time frame are used for calculating performance. Therefore the number of trials of each method is not necessarily equal to others.

significant performance degradation especially in Ant-fwd-bwd and Humanoid-direc. In Ant-fwd-bwd, the performance at $k = 100$ is significantly worse than that at $k = 10$. In Humanoid-direc, the performance at $k = 5$ is significantly worse than that at $k = 1$ (i.e., the one described in Figure 2). As we have seen, the performance degradation in Humanoid-direc is more sensitive to the model-rollout length than that in Ant-fwd-bwd. One of the reasons for this is that the meta-model error in Humanoid-direc is larger than that in Ant-fwd-bwd (Figure 8 in the appendix).

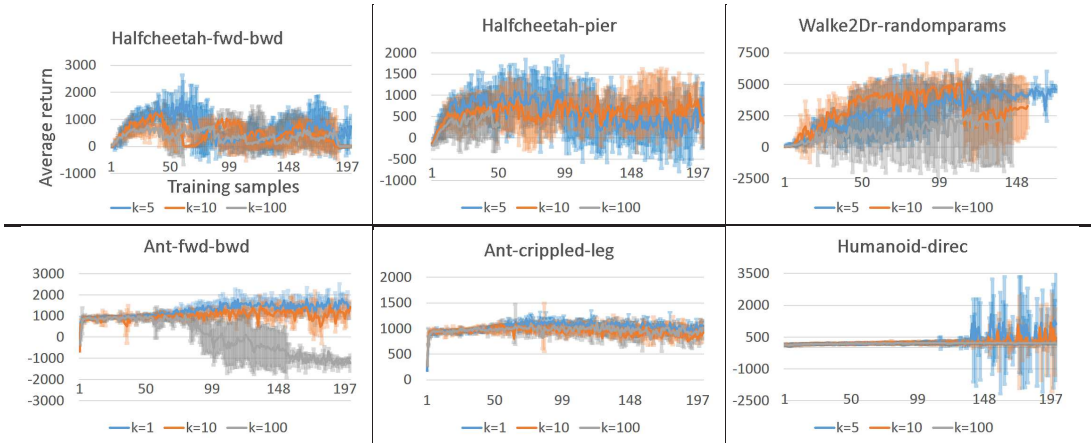


Figure 3: Learning curves of M3PO. In each figure, the vertical axis represents returns, and the horizontal axis represents numbers of training samples (x1000). The meta-policy and meta-model are fixed and evaluated their expected returns on 50 episodes per 1000 training samples. We run experiments by varying the rollout length k of M3PO. In these experiments, the values of hyperparameters except k are the same as those described in Table 1. Each case is evaluated at least in five trials, and the expected return on the 50 episodes is further averaged over the trials. The averaged expected returns and their standard deviations are plotted in the figures.

8 Conclusion

In this paper, we analyzed the performance guarantee (and performance degradation) of model-based RL in a meta-learning setting. We first formulated model-based reinforcement learning in a meta-learning setting as solving a POMDP. We then conducted theoretical analysis on the performance guarantee under both the full model-based rollout case and the branched meta-rollout case. Based on the theoretical result, we introduced branched meta-rollouts to policy optimization and proposed M3PO. Our experimental results show that it achieves better sample efficiency than a variant of PEARL and L2A. We also discussed important future work for improving M3PO (e.g., study on dynamic switching from M3PO to model-free approaches).

The statements of broader impact

Our work contributes to reducing various sorts of costs for training adaptive policies. The reduction of the costs enables us to apply RL to many practical problems where the costs had been a bottleneck on the application of RL. Such practical problems should contain ones where people are included as a part of environments and agents has a chance to harm them.

We encourage researchers and engineers to pay more attention to the safety aspect when they use RL methods for solving such problems.

References

- [1] Al-Shedivat, M., Bansal, T., Burda, Y., Sutskever, I., Mordatch, I., and Abbeel, P. Continuous adaptation via meta-learning in nonstationary and competitive environments. In Proc. ICLR, 2018.
- [2] Cho, K., Van Merriënboer, B., Gulcehre, C., Bahdanau, D., Bougares, F., Schwenk, H., and Bengio, Y. Learning phrase representations using RNN encoder-decoder for statistical machine translation. In Proc. EMNLP, 2014.
- [3] Clavera, I., Rothfuss, J., Schulman, J., Fujita, Y., Asfour, T., and Abbeel, P. Model-based reinforcement learning via meta-policy optimization. In Proc. CoRL, pp. 617–629, 2018.
- [4] Duan, Y., Schulman, J., Chen, X., Bartlett, P. L., Sutskever, I., and Abbeel, P. RL^2 : Fast reinforcement learning via slow reinforcement learning. In Proc. ICLR, 2017.
- [5] Feinberg, V., Wan, A., Stoica, I., Jordan, M. I., Gonzalez, J. E., and Levine, S. Model-based value expansion for efficient model-free reinforcement learning. In Proc. ICML, 2018.
- [6] Finn, C. and Levine, S. Meta-learning and universality: Deep representations and gradient descent can approximate any learning algorithm. In Proc. ICLR, 2018.
- [7] Finn, C., Abbeel, P., and Levine, S. Model-agnostic meta-learning for fast adaptation of deep networks. In Proc. ICML, pp. 1126–1135, 2017.
- [8] Ghavamzadeh, M., Mannor, S., Pineau, J., Tamar, A., et al. Bayesian reinforcement learning: A survey. Foundations and Trends® in Machine Learning, 8(5-6):359–483, 2015.
- [9] Gu, S., Holly, E., Lillicrap, T., and Levine, S. Deep reinforcement learning for robotic manipulation with asynchronous off-policy updates. In Proc. ICRA, pp. 3389–3396. IEEE, 2017.
- [10] Gupta, A., Mendonca, R., Liu, Y., Abbeel, P., and Levine, S. Meta-reinforcement learning of structured exploration strategies. In Proc. NeurIPS, pp. 5302–5311, 2018.
- [11] Haarnoja, T., Zhou, A., Abbeel, P., and Levine, S. Soft actor-critic: Off-policy maximum entropy deep reinforcement learning with a stochastic actor. In Proc. ICML, pp. 1856–1865, 2018.
- [12] Henaff, M. Explicit explore-exploit algorithms in continuous state spaces. In Proc. NeurIPS, 2019.
- [13] Hiraoka, T., Imagawa, T., Mori, T., Onishi, T., and Tsuruoka, Y. Learning robust options by conditional value at risk optimization. In Proc. NeurIPS, 2019.
- [14] Igl, M., Zintgraf, L., Le, T. A., Wood, F., and Whiteson, S. Deep variational reinforcement learning for POMDPs. In Proc. ICML, pp. 2117–2126, 2018.
- [15] Janner, M., Fu, J., Zhang, M., and Levine, S. When to trust your model: Model-based policy optimization. In Proc. NeurIPS, 2019.
- [16] Lee, A. X., Nagabandi, A., Abbeel, P., and Levine, S. Stochastic latent actor-critic: Deep reinforcement learning with a latent variable model. arXiv preprint arXiv:1907.00953, 2019.

- [17] Luo, Y., Xu, H., Li, Y., Tian, Y., Darrell, T., and Ma, T. Algorithmic framework for model-based deep reinforcement learning with theoretical guarantees. In Proc. ICLR, 2018.
- [18] Mendonca, R., Gupta, A., Kravev, R., Abbeel, P., Levine, S., and Finn, C. Guided meta-policy search. In Proc. NeurIPS, pp. 9653–9664, 2019.
- [19] Mishra, N., Rohaninejad, M., Chen, X., and Abbeel, P. A simple neural attentive meta-learner. In Proc. ICLR, 2018.
- [20] Mnih, V., Kavukcuoglu, K., Silver, D., Rusu, A. A., Veness, J., Bellemare, M. G., Graves, A., Riedmiller, M., Fidjeland, A. K., Ostrovski, G., et al. Human-level control through deep reinforcement learning. Nature, 518(7540):529–533, 2015.
- [21] Nagabandi, A., Kahn, G., Fearing, R. S., and Levine, S. Neural network dynamics for model-based deep reinforcement learning with model-free fine-tuning. In Proc. ICRA, pp. 7559–7566, 2018.
- [22] Nagabandi, A., Clavera, I., Liu, S., Fearing, R. S., Abbeel, P., Levine, S., and Finn, C. Learning to adapt in dynamic, real-world environments via meta-reinforcement learning. In Proc. ICLR, 2019.
- [23] Nagabandi, A., Finn, C., and Levine, S. Deep online learning via meta-learning: Continual adaptation for model-based RL. In Proc. ICLR, 2019.
- [24] Rajeswaran, A., Ghotra, S., Levine, S., and Ravindran, B. EPOpt: Learning Robust Neural Network Policies Using Model Ensembles. In Proc. ICLR, 2017.
- [25] Rajeswaran, A., Mordatch, I., and Kumar, V. A game theoretic framework for model based reinforcement learning, 2020.
- [26] Rakelly, K., Zhou, A., Finn, C., Levine, S., and Quillen, D. Efficient off-policy meta-reinforcement learning via probabilistic context variables. In Proc. ICML, pp. 5331–5340, 2019.
- [27] Rothfuss, J., Lee, D., Clavera, I., Asfour, T., and Abbeel, P. Prompt: Proximal meta-policy search. In Proc. ICLR, 2019.
- [28] Sæmundsson, S., Hofmann, K., and Deisenroth, M. P. Meta reinforcement learning with latent variable Gaussian processes. arXiv preprint arXiv:1803.07551, 2018.
- [29] Schmidhuber, J., Zhao, J., and Wiering, M. Simple principles of metalearning. Technical report IDSIA, 69:1–23, 1996.
- [30] Silver, D. and Veness, J. Monte-Carlo planning in large POMDPs. In Proc. NIPS, pp. 2164–2172, 2010.
- [31] Stadie, B. C., Yang, G., Houthoofd, R., Chen, X., Duan, Y., Wu, Y., Abbeel, P., and Sutskever, I. Some considerations on learning to explore via meta-reinforcement learning. arXiv preprint arXiv:1803.01118, 2018.
- [32] Sun, W. Towards Generalization and Efficiency in Reinforcement Learning. PhD thesis, Carnegie Mellon University, 2019.
- [33] Sun, W., Jiang, N., Krishnamurthy, A., Agarwal, A., and Langford, J. Model-based RL in contextual decision processes: PAC bounds and exponential improvements over model-free approaches. In Proc. COLT, pp. 2898–2933, 2019.
- [34] Sutton, R. S. Integrated architectures for learning, planning, and reacting based on approximating dynamic programming. In Proc. ML, pp. 216–224. Elsevier, 1990.
- [35] Thrun, S. and Pratt, L. Learning to learn: Introduction and overview. In science & business media, pp. 3–17. Springer, 1998.
- [36] Todorov, E., Erez, T., and Tassa, Y. Mujoco: A physics engine for model-based control. In Proc. IROS, pp. 5026–5033. IEEE, 2012.

- [37] Wang, J. X., Kurth-Nelson, Z., Tirumala, D., Soyer, H., Leibo, J. Z., Munos, R., Blundell, C., Kumaran, D., and Botvinick, M. Learning to reinforcement learn. [arXiv preprint arXiv:1611.05763](#), 2016.
- [38] Williams, G., Aldrich, A., and Theodorou, E. Model predictive path integral control using covariance variable importance sampling. [arXiv preprint arXiv:1509.01149](#), 2015.
- [39] Yu, T., Quillen, D., He, Z., Julian, R., Hausman, K., Finn, C., and Levine, S. Meta-world: A benchmark and evaluation for multi-task and meta reinforcement learning. In [Proc. CoRL](#), 2019.
- [40] Zintgraf, L., Shiarlis, K., Igl, M., Schulze, S., Gal, Y., Hofmann, K., and Whiteson, S. VariBAD: A very good method for Bayes-adaptive deep RL via meta-learning. In [Proc. ICLR](#), 2020.

A Appendices

A.1 How does our work differ from Janner et al.’s work [15]?

Although our work is grounded primarily on the basis of Janner et al.’s work [15], we provide non-trivial contributions in both theoretical and practical frontiers: **(1)** We provide theorems about the relation between true returns and returns on inaccurate predictive models (model returns) on a “meta-learning (POMDPs)” setting (Section 5). In their work, they provide theorems about the relation between the true returns and the model returns in the branched rollout in MDPs. In contrast, we provide theorems about the relation between the true returns and of the model returns in the branched rollout in POMDPs. *In addition, in the derivation of theorems (Theorems 4.2 and 4.3) in their work, a number of important premises are not properly taken into consideration* (the detailed discussion on it is described in the second paragraph in A.5). We provide new theorems, in which the premises are more properly reflected, for both MDPs and POMDPs (A.2 and A.5). **(2)** We extend the model-based policy optimization (MBPO) proposed by Janner et al. into the meta-learning (POMDPs) setting (Section 6). MBPO is for the MDP settings and does not support POMDP settings, while our method (M3PO) supports POMDP settings. Furthermore, we empirically demonstrate the usefulness of the meta-model usage in the branched rollout manner in the POMDP settings (Section 7).

A.2 Proofs of theorems in the main content

Before starting the derivation of the main theorems, we introduce a lemma useful for bridging POMDPs and MDPs.

Lemma 1 ([30]). *Given a POMDP $\langle \mathcal{O}, \mathcal{S}, \mathcal{A}, p_{ob}, r, \gamma, p_{st} \rangle$, consider the derived MDP with histories as states, $\langle \mathcal{H}, \mathcal{A}, \gamma, \bar{r}, p_{hi} \rangle$, where $\forall t. p_{hi} := p(h_{t+1}|a_{t+1}, h_t) = \sum_{s_t \in \mathcal{S}} \sum_{s_{t+1} \in \mathcal{S}} p(s_t|h_t)p(s_{t+1}|s_t, a_t)p(o_{t+1}|s_{t+1}, a_t)$ and $\bar{r}(h_t, a_t) := \sum_{s_t \in \mathcal{S}} p(s_t|h_t)r(s_t, a_t)$. Then, the value function $\bar{V}_\pi(h_t)$ of the derived MDP is equal to the value function $V_\pi(h_t)$ of the POMDP.*

Proof. The statement can be derived by backward induction on the value functions. See the proof of Lemma 1 in [30] for details. \square

Proof of Theorem 1:

Proof. By Lemma 1, our problem in POMDPs can be mapped into the problem in MDPs, and then Theorem 4.1 in [15] can be applied to the problem. \square

Similarly, the proofs of Theorems 2 and 3 are derived by mapping our problem into that in MDPs by Lemma 1 and leveraging theoretical results on MDPs.

Proof of Theorem 2:

Proof. By Lemma 1, our problem in POMDPs can be mapped into the problem in MDPs, and then Theorem 4 in A.5 can be applied to the problem. \square

Proof of Theorem 3:

Proof. By Lemma 1, our problem in POMDPs can be mapped into the problem in MDPs, and then Theorem 5 in A.5 can be applied to the problem. \square

A.3 The discrepancy relying on the meta-model error in Theorem 1 and that in Theorem 2

Corollary 1. *The discrepancy factors relying on ϵ_m in Theorem 1, $C_{Th1,m}$, are equal to or larger than those relying on ϵ_m at $k = 1$ in Theorem 2, $C_{Th2,m}$.*

Proof. By Theorem 1 and 2,

$$C_{Th1,m} = r_{\max} \frac{2\gamma\epsilon_m}{(1-\gamma)^2}. \quad (4)$$

$$C_{\text{Th2},m} = r_{\max} \frac{\gamma}{1-\gamma} 2\epsilon_m. \quad (5)$$

Given that $\gamma \in [0, 1)$, $r_{\max} > 0$ and $\epsilon_m \geq 0$,

$$\begin{aligned} C_{\text{Th1},m} - C_{\text{Th2},m} &= r_{\max} \frac{4\gamma\epsilon_m - 2\gamma^2\epsilon_m}{(1-\gamma)^2} \\ &\geq 0. \end{aligned} \quad (6)$$

□

A.4 Connection to a typical meta-RL setting

In Section 4, we formulate meta-model-based RL to solve a POMDP. However, this formulation may make it difficult for certain readers to comprehend the connection to a typical meta-RL setting. Although in the normative meta-RL setting (e.g., [7]), the objective to be optimized is given as the return expected with respect to a task distribution, such an objective does not appear in the formulation in Section 4. In this section, we show that such an objective can be derived by specializing the formulation in Section 4 under a number of assumptions (Corollary 2). Then, we explain why we did not adopt such a specialization and maintained a more abstract formulation in Section 4.

First, letting a task set and a task distribution be denoted by \mathcal{T} and $p(\tau)$ where $\tau \in \mathcal{T}$, respectively, we introduce the following assumptions:

Assumption 2. $\mathcal{S} := \mathcal{O} \times \mathcal{T}$.

Assumption 3. $p(s_{t+1}|s_t, a_t) := p(o_{t+1}|o_t, \tau_t, a_t) \cdot \mathbf{I}(\tau_{t+1} = \tau_t)$.

Assumption 4. For $t > 0$, $p(s_t|h_t) := p(\tau_t|h_t) \cdot \mathbf{I}(\tau_t = \tau_0)$.

Assumption 5. $p(\tau_0|h_0) := p(\tau_0)$.

With these assumptions, the following corollary holds:

Corollary 2. Given a POMDP $\langle \mathcal{O}, \mathcal{S}, \mathcal{A}, p_{\text{ob}}, r, \gamma, p_{\text{st}} \rangle$ and a task set \mathcal{T} , consider the parameterized MDP with histories as states, $\langle \mathcal{H}, \mathcal{A}, \gamma, \bar{r}, \bar{p}_{\text{ob}} \rangle$, where $\forall t$. $\bar{p}_{\text{ob}} := p(o_{t+1}|o_t, \tau_0, a_t)$ and $\bar{r} := r(o_t, \tau_0, a_t)$. Under Assumptions 2~5, the expected return on the parameterized MDP $\mathbb{E}_{a \sim \pi, h \sim p, \tau \sim p(\tau)} [\sum_t^\infty \gamma^t \bar{r}_t] := \sum_{\tau \in \mathcal{T}} p(\tau) \mathbb{E}_{a \sim \pi, h \sim p} [\sum_t^\infty \gamma^t \bar{r}_t | \tau]$ is equal to the expected return on the POMDP $\mathbb{E}_{a \sim \pi, h \sim p} [R]$.

Proof. By applying Lemma 1, the value function in a POMDP $\langle \mathcal{O}, \mathcal{S}, \mathcal{A}, p_{\text{ob}}, r, \gamma, p_{\text{st}} \rangle$ can be mapped to the value function $\bar{V}_\pi(h_t)$ in the derived MDP, which is $\langle \mathcal{H}, \mathcal{A}, \gamma, \bar{r}, p_{\text{hi}} \rangle$, where $\forall t$. $p_{\text{hi}} := p(h_{t+1}|a_{t+1}, h_t) = \sum_{s_t \in \mathcal{S}} \sum_{s_{t+1} \in \mathcal{S}} p(s_t|h_t) p(s_{t+1}|s_t, a_t) p(o_{t+1}|s_{t+1}, a_t)$ and $\bar{r}(h_t, a_t) := \sum_{s_t \in \mathcal{S}} p(s_t|h_t) r(s_t, a_t)$.

By applying the assumptions, this value function can be transformed to a different representation that explicitly contains τ and its distribution:

For $t > 0$,

$$\begin{aligned} \bar{V}_\pi(h_t) &= \sum_{a_{t+1}} \pi(a_{t+1}|h_t) \left\{ \sum_{s_t \in \mathcal{S}} p(s_t|h_t) r(s_t, a_t) \right. \\ &\quad \left. + \gamma \sum_{o_{t+1} \in \mathcal{O}} \sum_{s_t \in \mathcal{S}} \sum_{s_{t+1} \in \mathcal{S}} p(s_t|h_t) p(s_{t+1}|s_t, a_t) p(o_{t+1}|s_{t+1}, a_t) \bar{V}_\pi(h_{t+1}) \right\} \\ &= \sum_{a_{t+1}} \pi(a_{t+1}|h_t) \left\{ \underbrace{r(o_t, \tau_0, a_t)}_{\bar{r}_t} + \gamma \sum_{o_{t+1} \in \mathcal{O}} \underbrace{p(o_{t+1}|o_t, \tau_0, a_t)}_{\bar{p}_{\text{ob}}} \bar{V}_\pi(h_{t+1}) \right\}. \end{aligned} \quad (7)$$

Likewise, for $t = 0$,

$$\begin{aligned}\bar{V}_\pi(h_0) &= \sum_{a_1} \pi(a_1|h_0) \left\{ \sum_{\tau_0} p(\tau_0) r(o_0, \tau_0, a_0) + \gamma \sum_{o_1 \in \mathcal{O}} \sum_{\tau_0} p(\tau_0) p(o_1|o_0, \tau_0, a_0) \bar{V}_\pi(h_1) \right\} \\ &= \sum_{\tau_0} p(\tau_0) \underbrace{\sum_{a_1} \pi(a_1|h_0) \left\{ r(o_0, \tau_0, a_0) + \gamma \sum_{o_1 \in \mathcal{O}} p(o_1|o_0, \tau_0, a_0) \bar{V}_\pi(h_1) \right\}}_{\bar{V}_\pi(h_0)}.\end{aligned}\quad (8)$$

Therefore,

$$\begin{aligned}\mathbb{E}_{a \sim \pi, h \sim p}[R] &= \sum_{h_0} p(h_0) \bar{V}_\pi(h_0) \\ &= \sum_{\tau_0} p(\tau_0) \sum_{h_0} p(h_0) \bar{V}_\pi(h_0) \\ &= \mathbb{E}_{a \sim \pi, h \sim p, \tau \sim p(\tau)} \left[\sum_t^\infty \gamma^t \bar{r}_t \right]\end{aligned}\quad (9)$$

□

By Corollary 2, our formulation in Section 4 can be specialized into a problem where the objective to be optimized is given as the return expected with respect to a task distribution. We can derive the meta-model returns with discrepancies for bounding the true return (i.e., $\mathbb{E}_{a \sim \pi_\phi, h \sim p_\theta, \tau \sim p(\tau)} [\sum_t^\infty \gamma^t \bar{r}_t] - C(\epsilon_m, \epsilon_\pi)$) by using Corollary 2 instead of Lemma 1 in the proofs of Theorem 1 and replacing $p_\theta(o_t|o_0, \tau_0, a_t)$ with $p_\theta(o_t|h_{t-1})$.

The main reason that we do not adopt such a specialization in Section 4 is to avoid restrictions induced by the assumptions (Assumption 2~5). For example, Assumption 2 states that hidden states are composed by observations and a task. Since observations can be observed from an agent by its definition, the information in the hidden states that cannot be observed from an agent is the task. However, in many meta-RL settings (e.g., application domains where video images are used as the observation), there should be other information that cannot be observed from the agent. In addition, Assumptions 3 and 4 state that the task is invariant in each episode. However, in many meta-RL settings (e.g., [22, 23]), the task can change to a different one in each episode. To avoid such restrictions, we decided not to specialize the formulation by introducing the assumptions.

A.5 The derivation of the relation of the returns in k -step branched rollouts ($k \geq 1$) in Markov decision processes

In this section, we discuss the relation of the true returns and the model returns under the branched rollout in an MDP, which is defined by a tuple $\langle \mathcal{S}, \mathcal{A}, r, \gamma, p_{\text{st}} \rangle$. Here, \mathcal{S} is the set of states, \mathcal{A} is the set of actions, $p_{\text{st}} := p(s'|s, a)$ is the state transition probability for any $s', s \in \mathcal{S}$ and $a \in \mathcal{A}$, r is the reward function and $\gamma \in [0, 1]$ is the discount factor. At time step t , the former two functions are used as $p(s_t|s_{t-1}, a_t)$, $r_t = r(s_t, a_t)$. The agent selects an action on the basis of a policy $\pi := p(a_{t+1}|s_t)$. We denote the data collection policy by $\pi_{\mathcal{D}}$ and the state visitation probability under $\pi_{\mathcal{D}}$ and $p(s'|s, a)$ by $p_{\pi_{\mathcal{D}}}(s_t)$. We also denote the predictive model for the next state by $p_\theta(s'|s, a)$. In addition, we define the upper bounds of the reward scale as $r_{\max} > \max_{s,a} |r(s, a)|$. Note that, in this section, to discuss the MDP case, we are overriding the definition of the variables and functions that were defined for the POMDP case in the main body. In addition, for simplicity, we use the abbreviated style $\mathbb{E}_{\pi, p}[R]$ for the true return $\mathbb{E}_{a \sim \pi, s \sim p}[R := \sum_{t=0}^\infty \gamma^t r_t]$.

Although the theoretical analysis on the relation of the returns in the MDP case is provided by Janner et al. [15], in their analysis, a number of important premises are not properly taken into consideration. First, although they use the replay buffers for the branched rollout (i.e. datasets \mathcal{D}_{env} and $\mathcal{D}_{\text{model}}$ in Algorithm 2 in [15]), they do not take the use of the replay buffers into account in their theoretical analysis. Furthermore, they calculate state-action visitation probabilities based solely on a single

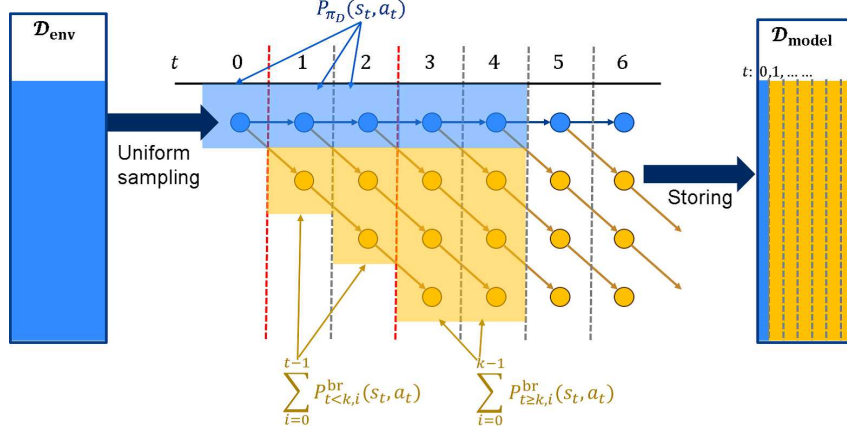


Figure 4: An example of branched rollouts with $k = 3$. Here, the blue dots represent trajectories contained in an environment dataset \mathcal{D}_{env} and the yellow dots represent fictitious trajectories generated in accordance with a current policy π under a predictive model p_θ .

model-based rollout factor. In the branched rollout, state-action visitation probabilities (except for the one at $t = 0$) should be affected by multiple past model-based rollouts. For example, a state-action visitation probability at t (s.t. $t > k$) is affected by the model-based rollout branched from real trajectories at $t - k$ and ones from $t - k + 1$ to $t - 1$ (in total, k model-based rollouts). However, in their analysis (the proof of Lemma B.4 in [15]), they calculate state-action visitation probabilities based solely on the model-based rollout. For example, in their analysis, it is assumed that a state-action visitation probability at t (s.t. $t > k$) is affected only by the model-based rollout branched from real trajectories at $t - k$. These oversights of important premises in their analysis induce a large mismatch between those for their theorems and those made for the actual implementation of the branched rollout (i.e., Algorithm 2 in [15]). Therefore, we decided to newly derive the theorems on the branched rollout, reflecting these premises more appropriately.

The outline of our branched rollout is shown in Figure 4. Here, we assume that the trajectories collected from the real environment are stored in a dataset \mathcal{D}_{env} . The trajectories stored in \mathcal{D}_{env} can be seen as trajectories following the true dynamics $p(s'|s, a)$ and data collection policy (i.e., a mixture of previous policies used for data collection) $\pi_{\mathcal{D}}$. At each branched rollout, the trajectories in \mathcal{D}_{env} are uniformly sampled¹¹, and then starting from the sampled trajectories, k -step model-based rollouts in accordance with π under p_θ is run. The fictitious trajectories generated by the branched rollout is stored in a model dataset $\mathcal{D}_{\text{model}}$ ¹². This process more appropriately reflects the actual implementation of the branched rollout (i.e., lines 5–8 in Algorithm 2) in [15]¹³. The performance of π is evaluated as the expected return under the state-action visitation probability in $\mathcal{D}_{\text{model}}$.

¹¹Thus, the initial state probability for the rollout starting from the trajectories follows $p_{\pi_{\mathcal{D}}}(s)$

¹²Here, when the trajectories are stored in $\mathcal{D}_{\text{model}}$, the states in the trajectories are augmented with time step information to deal with the state transition depending on the time step.

¹³Note that the extension of this process to the POMDP case is compatible with the implementation of the branched meta-rollout in our algorithm (lines 4–13 in Algorithm 2).

Formally, we define the return in the branched rollout $\mathbb{E}_{(a,s) \sim \mathcal{D}_{\text{model}}}[R]$ as:

$$\begin{aligned} \mathbb{E}_{(a,s) \sim \mathcal{D}_{\text{model}}}[R] &:= \sum_{s_0, a_0} p_{\pi_{\mathcal{D}}}(s_0, a_0) r(s_0, a_0) + \sum_{t=1}^{k-1} \sum_{s_t, a_t} \gamma^t p_{t < k}^{\text{br}}(s_t, a_t) r(s_t, a_t) \\ &\quad + \sum_{t=k}^{\infty} \sum_{s_t, a_t} \gamma^t p_{t \geq k}^{\text{br}}(s_t, a_t) r(s_t, a_t) \end{aligned} \quad (10)$$

$$p_{t < k}^{\text{br}}(s_t, a_t) := \frac{1}{t} \sum_{i=0}^{t-1} p_{t < k, i}^{\text{br}}(s_t, a_t) \quad (11)$$

$$p_{t \geq k}^{\text{br}}(s_t, a_t) := \frac{1}{k} \sum_{i=0}^{k-1} p_{t \geq k, i}^{\text{br}}(s_t, a_t) \quad (12)$$

$$p_{t < k, i}^{\text{br}}(s_t, a_t) := \sum_{s_i, \dots, s_{t-1}} \sum_{a_i, \dots, a_{t-1}} p_{\pi_{\mathcal{D}}}(s_i) \prod_{j=i}^{t-1} p_{\theta}(s_{j+1} | s_j, a_{j+1}) \pi(a_{j+1} | s_j) \quad (13)$$

$$\begin{aligned} p_{t \geq k, i}^{\text{br}}(s_t, a_t) &:= \sum_{s_{t-k+i}, \dots, s_{t-1}} \sum_{a_{t-k+i}, \dots, a_{t-1}} \\ &\quad p_{\pi_{\mathcal{D}}}(s_{t-k+i}) \prod_{j=t-k+i}^{t-1} p_{\theta}(s_{j+1} | s_j, a_{j+1}) \pi(a_{j+1} | s_j) \end{aligned} \quad (14)$$

Here, $p_{t < k, i}^{\text{br}}(s_t, a_t)$ and $p_{t \geq k, i}^{\text{br}}(s_t, a_t)$ are the state-action visitation probabilities that the i -th yellow trajectories (node) from the bottom at each timestep t in Figure 4 follow. In later discussions, for simplicity, we use the abbreviated style $\mathbb{E}_{\mathcal{D}_{\text{model}}}[R]$ for $\mathbb{E}_{(a,s) \sim \mathcal{D}_{\text{model}}}[R]$.

Before starting the derivation of theorems, we introduce a useful lemma.

Lemma 2. *Assume that the rollout process in which the policy and dynamics can be switched to other ones at time step t_{sw} . Letting two probabilities be p_1 and p_2 , for $1 \leq t' \leq t_{\text{sw}}$, we assume that the dynamics distributions are bounded as $\epsilon_{m, \text{pre}} \geq \max_{t'} E_{s \sim p_1} [D_{\text{TV}}(p_1(s_{t'} | s_{t'-1}, a_{t'}) || p_2(s_{t'} | s_{t'-1}, a_{t'}))]$. In addition, for $t_{\text{sw}} < t' \leq t$, we assume that the dynamics distributions are bounded as $\epsilon_{m, \text{post}} \geq \max_{t'} E_{s \sim p_1} [D_{\text{TV}}(p_1(s_{t'} | s_{t'-1}, a_{t'}) || p_2(s_{t'} | s_{t'-1}, a_{t'}))]$. Likewise, the policy divergence is bounded by $\epsilon_{\pi, \text{pre}}$ and $\epsilon_{\pi, \text{post}}$. Then, the following inequation holds*

$$\sum_{s_t, a_t} |p_1(s_t, a_t) - p_2(s_t, a_t)| \leq 2(t - t_{\text{sw}})(\epsilon_{m, \text{post}} + \epsilon_{\pi, \text{post}}) + 2t_{\text{sw}}(\epsilon_{m, \text{pre}} + \epsilon_{\pi, \text{pre}}) \quad (15)$$

Proof. The proof is done in a similar manner to those of Lemma B.1 and B.2 in [15].

$$\begin{aligned}
& \sum_{s_t, a_t} |p_1(s_t, a_t) - p_2(s_t, a_t)| \\
&= \sum_{s_t, a_t} |p_1(a_t)p_1(s_t|a_t) - p_2(a_t)p_2(s_t|a_t)| \\
&= \sum_{s_t, a_t} |p_1(a_t)p_1(s_t|a_t) - p_1(a_t)p_2(s_t|a_t) + (p_1(a_t) - p_2(a_t))p_2(s_t|a_t)| \\
&\leq \sum_{s_t, a_t} p_1(a_t) |p_1(s_t|a_t) - p_2(s_t|a_t)| + \sum_{a_t} |p_1(a_t) - p_2(a_t)| \\
&\leq \sum_{s_t, a_t} p_1(a_t) |p_1(s_t|a_t) - p_2(s_t|a_t)| + \sum_{a_t, s_{t-1}} |p_1(a_t, s_{t-1}) - p_2(a_t, s_{t-1})| \\
&= \sum_{s_t, a_t} p_1(a_t) |p_1(s_t|a_t) - p_2(s_t|a_t)| \\
&\quad + \sum_{a_t, s_{t-1}} |p_1(s_{t-1})p_1(a_t|s_{t-1}) - p_1(s_{t-1})p_2(a_t|s_{t-1}) + (p_1(s_{t-1}) - p_2(s_{t-1}))p_2(a_t|s_{t-1})| \\
&\leq \sum_{s_t, a_t} p_1(a_t) |p_1(s_t|a_t) - p_2(s_t|a_t)| + \sum_{a_t, s_{t-1}} p_1(s_{t-1}) |p_1(a_t|s_{t-1}) - p_2(a_t|s_{t-1})| \\
&\quad + \sum_{s_{t-1}} |p_1(s_{t-1}) - p_2(s_{t-1})| \\
&\leq \sum_{s_t, a_t} p_1(a_t) |p_1(s_t|a_t) - p_2(s_t|a_t)| + \sum_{a_t, s_{t-1}} p_1(s_{t-1}) |p_1(a_t|s_{t-1}) - p_2(a_t|s_{t-1})| \\
&\quad + \sum_{s_{t-1}, a_{t-1}} |p_1(s_{t-1}, a_{t-1}) - p_2(s_{t-1}, a_{t-1})| \\
&\leq 2\epsilon_{m, \text{post}} + 2\epsilon_{\pi, \text{post}} + \sum_{s_{t-1}, a_{t-1}} |p_1(s_{t-1}, a_{t-1}) - p_2(s_{t-1}, a_{t-1})| \\
&\leq 2(t - t_{\text{sw}})(\epsilon_{m, \text{post}} + \epsilon_{\pi, \text{post}}) + \sum_{s_{t_{\text{sw}}}, a_{t_{\text{sw}}}} |p_1(s_{t_{\text{sw}}}, a_{t_{\text{sw}}}) - p_2(s_{t_{\text{sw}}}, a_{t_{\text{sw}}})| \\
&\leq 2(t - t_{\text{sw}})(\epsilon_{m, \text{post}} + \epsilon_{\pi, \text{post}}) + 2t_{\text{sw}}(\epsilon_{m, \text{pre}} + \epsilon_{\pi, \text{pre}})
\end{aligned} \tag{16}$$

□

Now, we start the derivation of our bounds.

Theorem 4. *Under the k -step branched rollouts, using the bound of a model error under $\pi_{\mathcal{D}}$, $\epsilon_m = \max_t \mathbb{E}_{a \sim \pi_{\mathcal{D}}, s \sim p, t} [D_{TV}(p(s'|s, a) || p_{\theta}(s'|s, a))]$ and the bound of the policy shift $\epsilon_{\pi} = \max_s D_{TV}(\pi || \pi_{\mathcal{D}})$, the following inequation holds,*

$$\begin{aligned}
\mathbb{E}_{\pi, p} [R] &\geq \mathbb{E}_{\mathcal{D}_{\text{model}}} [R] - r_{\max} \left\{ \frac{1 + \gamma^2}{(1 - \gamma)^2} 2\epsilon_{\pi} + \frac{\gamma - k\gamma^k + (k - 1)\gamma^{k+1}}{(1 - \gamma)^2} (\epsilon_{\pi} + \epsilon_m) \right. \\
&\quad \left. + \frac{\gamma^k - \gamma}{\gamma - 1} (\epsilon_{\pi} + \epsilon_m) + \frac{\gamma^k}{1 - \gamma} (k + 1) (\epsilon_{\pi} + \epsilon_m) \right\}.
\end{aligned} \tag{17}$$

Proof.

$$\begin{aligned}
|\mathbb{E}_{\pi,p}[R] - \mathbb{E}_{\mathcal{D}_{\text{model}}}[R]| &= \left| \sum_{s_0,a_0} \{p_\pi(s_0,a_0) - p_{\pi_{\mathcal{D}}}(s_0,a_0)\} r(s_0,a_0) \right. \\
&\quad \left. + \sum_{t=1}^{k-1} \sum_{s_t,a_t} \gamma^t \{p_\pi(s_t,a_t) - p_{t<k}^{\text{br}}(s_t,a_t)\} r(s_t,a_t) \right. \\
&\quad \left. + \sum_{t=k}^{\infty} \sum_{s_t,a_t} \gamma^t \{p_\pi(s_t,a_t) - p_{t\geq k}^{\text{br}}(s_t,a_t)\} r(s_t,a_t) \right| \\
&\leq \left\{ \sum_{s_0,a_0} |p_\pi(s_0,a_0) - p_{\pi_{\mathcal{D}}}(s_0,a_0)| |r(s_0,a_0)| \right. \\
&\quad \left. + \sum_{t=1}^{k-1} \gamma^t \sum_{s_t,a_t} |p_\pi(s_t,a_t) - p_{t<k}^{\text{br}}(s_t,a_t)| |r(s_t,a_t)| \right. \\
&\quad \left. + \sum_{t=k}^{\infty} \gamma^t \sum_{s_t,a_t} |p_\pi(s_t,a_t) - p_{t\geq k}^{\text{br}}(s_t,a_t)| |r(s_t,a_t)| \right\} \\
&\leq \left\{ \underbrace{r_{\max} \sum_{s_0,a_0} |p_\pi(s_0,a_0) - p_{\pi_{\mathcal{D}}}(s_0,a_0)|}_{\text{term A}} \right. \\
&\quad \left. + r_{\max} \sum_{t=1}^{k-1} \gamma^t \underbrace{\sum_{s_t,a_t} |p_\pi(s_t,a_t) - p_{t<k}^{\text{br}}(s_t,a_t)|}_{\text{term B}} \right. \\
&\quad \left. + r_{\max} \sum_{t=k}^{\infty} \gamma^t \underbrace{\sum_{s_t,a_t} |p_\pi(s_t,a_t) - p_{t\geq k}^{\text{br}}(s_t,a_t)|}_{\text{term C}} \right\} \quad (18)
\end{aligned}$$

For **term A**, we can bound the value in similar manner to the derivation of Lemma 2.

$$\begin{aligned}
\sum_{s_0,a_0} |p_\pi(s_0,a_0) - p_{\pi_{\mathcal{D}}}(s_0,a_0)| &= \sum_{s_0,a_0} |p_\pi(a_0)p(s_0) - p_{\pi_{\mathcal{D}}}(a_0)p(s_0)| \\
&= \sum_{s_0,a_0} |p_\pi(a_0)p(s_0) - p_\pi(a_0)p(s_0) + (p_\pi(a_0) - p_{\pi_{\mathcal{D}}}(a_0))p(s_0)| \\
&\leq \underbrace{\sum_{s_0,a_0} p_\pi(a_0) |p(s_0) - p(s_0)|}_{=0} + \underbrace{\sum_{a_0} |p_\pi(a_0) - p_{\pi_{\mathcal{D}}}(a_0)|}_{\leq 2\epsilon_\pi} \\
&\leq 2\epsilon_\pi \quad (19)
\end{aligned}$$

For **term B**, we can apply Lemma 2 to bound the value, but it requires the bounded model error under the current policy π . Thus, we need to decompose the distance into two by adding and subtracting $p_{\pi_{\mathcal{D}}}$:

$$\begin{aligned}
\sum_{s_t,a_t} |p_\pi(s_t,a_t) - p_{t<k}^{\text{br}}(s_t,a_t)| &= \sum_{s_t,a_t} \left| \frac{p_\pi(s_t,a_t) - p_{\pi_{\mathcal{D}}}(s_t,a_t)}{+p_{\pi_{\mathcal{D}}}(s_t,a_t) - p_{t<k}^{\text{br}}(s_t,a_t)} \right| \\
&\leq \underbrace{\sum_{s_t,a_t} |p_\pi(s_t,a_t) - p_{\pi_{\mathcal{D}}}(s_t,a_t)|}_{\leq 2t\epsilon_\pi} \\
&\quad + \sum_{s_t,a_t} |p_{\pi_{\mathcal{D}}}(s_t,a_t) - p_{t<k}^{\text{br}}(s_t,a_t)| \quad (20)
\end{aligned}$$

$$\begin{aligned}
\sum_{s_t,a_t} |p_{\pi_{\mathcal{D}}}(s_t,a_t) - p_{t<k}^{\text{br}}(s_t,a_t)| &= \sum_{s_t,a_t} \left| \frac{1}{t} \sum_{i=0}^{t-1} p_{\pi_{\mathcal{D}}}(s_t,a_t) - \frac{1}{t} \sum_{i=0}^{t-1} p_{t<k,i}^{\text{br}}(s_t,a_t) \right| \\
&\leq \frac{1}{t} \sum_{i=0}^{t-1} \sum_{s_t,a_t} |p_{\pi_{\mathcal{D}}}(s_t,a_t) - p_{t<k,i}^{\text{br}}(s_t,a_t)| \\
&\stackrel{(A)}{\leq} \frac{1}{t} \sum_{i=0}^{t-1} \{2(t-i) \cdot (\epsilon_\pi + \epsilon_m)\} \\
&= \frac{1}{t} \{t^2(\epsilon_\pi + \epsilon_m) + t(\epsilon_\pi + \epsilon_m)\} \quad (21)
\end{aligned}$$

For (A), we apply Lemma 2 with setting $\epsilon_{m,\text{post}} = \epsilon_m$ and $\epsilon_{\pi,\text{post}} = \epsilon_\pi$ for the rollout following π and $p_\theta(s'|s)$, and $\epsilon_{m,\text{pre}} = 0$ and $\epsilon_{\pi,\text{pre}} = 0$ for the rollout following $\pi_{\mathcal{D}}$ and $p(s'|s)$, respectively. To recap **term B**, the following equation holds:

$$\sum_{s_t, a_t} |p_\pi(s_t, a_t) - p_{\text{br}, t < k}(s_t, a_t)| \leq 2t\epsilon_\pi + t(\epsilon_\pi + \epsilon_m) + (\epsilon_\pi + \epsilon_m) \quad (22)$$

For **term C**, we can derive the bound in a similar manner to the term B case:

$$\begin{aligned} \sum_{s_t, a_t} |p_\pi(s_t, a_t) - p_{\text{br}, t \geq k}(s_t, a_t)| &= \sum_{s_t, a_t} |p_\pi(s_t, a_t) - p_{\pi_{\mathcal{D}}}(s_t, a_t) + p_{\pi_{\mathcal{D}}}(s_t, a_t) - p_{t \geq k}^{\text{br}}(s_t, a_t)| \\ &\leq \underbrace{\sum_{s_t, a_t} |p_\pi(s_t, a_t) - p_{\pi_{\mathcal{D}}}(s_t, a_t)|}_{\leq 2t\epsilon_\pi} \\ &\quad + \sum_{s_t, a_t} |p_{\pi_{\mathcal{D}}}(s_t, a_t) - p_{t \geq k}^{\text{br}}(s_t, a_t)| \end{aligned} \quad (23)$$

$$\begin{aligned} \sum_{s_t, a_t} |p_{\pi_{\mathcal{D}}}(s_t, a_t) - p_{t \geq k}^{\text{br}}(s_t, a_t)| &= \sum_{s_t, a_t} \left| \frac{1}{k} \sum_{i=0}^{k-1} p_{\pi_{\mathcal{D}}}(s_t, a_t) - \frac{1}{k} \sum_{i=0}^{k-1} p_{t \geq k, i}^{\text{br}}(s_t, a_t) \right| \\ &\leq \frac{1}{k} \sum_{i=0}^{k-1} \sum_{s_t, a_t} |p_{\pi_{\mathcal{D}}}(s_t, a_t) - p_{t \geq k, i}^{\text{br}}(s_t, a_t)| \\ &\leq \frac{1}{k} \sum_{i=0}^{k-1} \{2(k-i) \cdot (\epsilon_\pi + \epsilon_m)\} \\ &= \frac{1}{k} \{k^2(\epsilon_\pi + \epsilon_m) + k(\epsilon_\pi + \epsilon_m)\} \end{aligned} \quad (24)$$

To recap **term C**, the following equation holds:

$$\sum_{s_t, a_t} |p_\pi(s_t, a_t) - p_{t \geq k}^{\text{br}}(s_t, a_t)| \leq 2t\epsilon_\pi + k(\epsilon_\pi + \epsilon_m) + (\epsilon_\pi + \epsilon_m) \quad (25)$$

By substituting Eqs. 19, 22, and 25, into Eq. 18, we obtain the result:

$$\begin{aligned}
|\mathbb{E}_{\pi,p}[R] - \mathbb{E}_{\mathcal{D}_{\text{model}}}[R]| &\leq \left\{ \begin{aligned} &r_{\max} 2\epsilon_{\pi} \\ &+ r_{\max} \sum_{t=k}^{\infty} \gamma^t \{2t\epsilon_{\pi} + t(\epsilon_{\pi} + \epsilon_m) + (\epsilon_{\pi} + \epsilon_m)\} \\ &+ r_{\max} \sum_{t=k}^{\infty} \gamma^t \{2t\epsilon_{\pi} + k(\epsilon_{\pi} + \epsilon_m) + (\epsilon_{\pi} + \epsilon_m)\} \end{aligned} \right\} \\
&= r_{\max} \left\{ \begin{aligned} &2\epsilon_{\pi} + \frac{1-k\gamma^{(k-1)}+(k-1)\gamma^k}{(1-\gamma)^2} \gamma (3\epsilon_{\pi} + \epsilon_m) + \frac{\gamma^k - \gamma}{\gamma - 1} (\epsilon_{\pi} + \epsilon_m) \\ &+ \sum_{t=k}^{\infty} \gamma^t \{2t\epsilon_{\pi} + k(\epsilon_{\pi} + \epsilon_m) + (\epsilon_{\pi} + \epsilon_m)\} \end{aligned} \right\} \\
&= r_{\max} \left\{ \begin{aligned} &2\epsilon_{\pi} + \frac{1-k\gamma^{(k-1)}+(k-1)\gamma^k}{(1-\gamma)^2} \gamma (3\epsilon_{\pi} + \epsilon_m) + \frac{\gamma^k - \gamma}{\gamma - 1} (\epsilon_{\pi} + \epsilon_m) \\ &+ \sum_{t=k}^{\infty} \gamma^t \{2t\epsilon_{\pi} + k(\epsilon_{\pi} + \epsilon_m) + (\epsilon_{\pi} + \epsilon_m)\} \\ &- \sum_{t=1}^{k-1} \gamma^t \{2t\epsilon_{\pi} + k(\epsilon_{\pi} + \epsilon_m) + (\epsilon_{\pi} + \epsilon_m)\} \end{aligned} \right\} \\
&= r_{\max} \left\{ \begin{aligned} &2\epsilon_{\pi} + \frac{1-k\gamma^{(k-1)}+(k-1)\gamma^k}{(1-\gamma)^2} \gamma (3\epsilon_{\pi} + \epsilon_m) + \frac{\gamma^k - \gamma}{\gamma - 1} (\epsilon_{\pi} + \epsilon_m) \\ &+ \frac{2}{(1-\gamma)^2} \gamma \epsilon_{\pi} + \frac{\gamma}{1-\gamma} \{k(\epsilon_{\pi} + \epsilon_m) + (\epsilon_{\pi} + \epsilon_m)\} \\ &- \sum_{t=1}^{k-1} \gamma^t \{2t\epsilon_{\pi} + k(\epsilon_{\pi} + \epsilon_m) + (\epsilon_{\pi} + \epsilon_m)\} \end{aligned} \right\} \\
&= r_{\max} \left\{ \begin{aligned} &2\epsilon_{\pi} + \frac{1-k\gamma^{(k-1)}+(k-1)\gamma^k}{(1-\gamma)^2} \gamma (3\epsilon_{\pi} + \epsilon_m) + \frac{\gamma^k - \gamma}{\gamma - 1} (\epsilon_{\pi} + \epsilon_m) \\ &+ \frac{2}{(1-\gamma)^2} \gamma \epsilon_{\pi} + \frac{\gamma}{1-\gamma} \{k(\epsilon_{\pi} + \epsilon_m) + (\epsilon_{\pi} + \epsilon_m)\} \\ &- \frac{1-k\gamma^{(k-1)}+(k-1)\gamma^k}{(1-\gamma)^2} 2\gamma \epsilon_{\pi} - \frac{\gamma^k - \gamma}{\gamma - 1} \{k(\epsilon_{\pi} + \epsilon_m) + (\epsilon_{\pi} + \epsilon_m)\} \end{aligned} \right\} \\
&= r_{\max} \left\{ \begin{aligned} &\frac{1+\gamma^2}{(1-\gamma)^2} 2\epsilon_{\pi} + \frac{\gamma - k\gamma^k + (k-1)\gamma^{k+1}}{(1-\gamma)^2} (\epsilon_{\pi} + \epsilon_m) \\ &+ \frac{\gamma^k - \gamma}{\gamma - 1} (\epsilon_{\pi} + \epsilon_m) + \left(\frac{\gamma}{1-\gamma} - \frac{\gamma^k - \gamma}{\gamma - 1} \right) (k+1)(\epsilon_{\pi} + \epsilon_m) \end{aligned} \right\} \\
&= r_{\max} \left\{ \begin{aligned} &\frac{1+\gamma^2}{(1-\gamma)^2} 2\epsilon_{\pi} + \frac{\gamma - k\gamma^k + (k-1)\gamma^{k+1}}{(1-\gamma)^2} (\epsilon_{\pi} + \epsilon_m) \\ &+ \frac{\gamma^k - \gamma}{\gamma - 1} (\epsilon_{\pi} + \epsilon_m) + \frac{\gamma^k}{1-\gamma} (k+1)(\epsilon_{\pi} + \epsilon_m) \end{aligned} \right\} \tag{26}
\end{aligned}$$

□

Theorem 5. Let $\epsilon_{m'} \geq \max_t E_{a \sim \pi, s \sim p}[D_{TV}(p(s'|s, a) || p_{\theta}(s'|s, a))]$,

$$\begin{aligned}
\mathbb{E}_{\pi,p}[R] \geq \mathbb{E}_{\mathcal{D}_{\text{model}}}[R] - r_{\max} \left\{ \begin{aligned} &\frac{1+\gamma^2}{(1-\gamma)^2} 2\epsilon_{\pi} + \frac{1-k\gamma^{(k-1)}+(k-1)\gamma^k}{(1-\gamma)^2} \gamma (\epsilon_{m'} - \epsilon_{\pi}) \\ &+ \frac{\gamma^k - \gamma}{\gamma - 1} (\epsilon_{m'} - \epsilon_{\pi}) + \frac{\gamma^k}{1-\gamma} (k+1)(\epsilon_{m'} - \epsilon_{\pi}) \end{aligned} \right\}. \tag{27}
\end{aligned}$$

Proof. The derivation of this theorem is basically the same as that in the Theorem 4 case except for the way of evaluation of the bound of terms B and C.

For **term B**, we can apply Lemma 2 to bound the value:

$$\begin{aligned}
\sum_{s_t, a_t} |p_{\pi}(s_t, a_t) - p_{t < k}^{\text{br}}(s_t, a_t)| &= \sum_{s_t, a_t} \left| \frac{1}{t} \sum_{i=0}^{t-1} p_{\pi_{\mathcal{D}}}(s_t, a_t) - \frac{1}{t} \sum_{i=0}^{t-1} p_{t < k, i}^{\text{br}}(s_t, a_t) \right| \\
&\leq \frac{1}{t} \sum_{i=0}^{t-1} \sum_{s_t, a_t} |p_{\pi}(s_t, a_t) - p_{t < k, i}^{\text{br}}(s_t, a_t)| \\
&\stackrel{(D)}{\leq} \frac{1}{t} \sum_{i=0}^{t-1} \{(t-i)2\epsilon_{m'} + i2\epsilon_{\pi}\} \\
&= \frac{1}{t} \{2t^2\epsilon_{m'} - (t-1)t\epsilon_{m'} + (t-1)t\epsilon_{\pi}\} \\
&= \frac{1}{t} \{2t^2\epsilon_{m'} - t^2\epsilon_{m'} + t\epsilon_{m'} + t^2\epsilon_{\pi} - t\epsilon_{\pi}\} \\
&= \frac{1}{t} \{t^2(\epsilon_{m'} + \epsilon_{\pi}) + t(\epsilon_{m'} - \epsilon_{\pi})\} \\
&= t(\epsilon_{m'} + \epsilon_{\pi}) + (\epsilon_{m'} - \epsilon_{\pi}) \tag{28}
\end{aligned}$$

For (D), we apply Lemma 2 with setting $\epsilon_{m,\text{post}} = \epsilon_{m'}$ and $\epsilon_{\pi,\text{post}} = 0$ for the rollout following π and $p_\theta(s'|s)$, and $\epsilon_{m,\text{pre}} = 0$ and $\epsilon_{\pi,\text{pre}} = \epsilon_\pi$ for the rollout following $\pi_{\mathcal{D}}$ and $p(s'|s)$.

For **term C**, we can derive the bound in a similar manner to the case of term B:

$$\begin{aligned}
\sum_{s_t, a_t} |p_\pi(s_t, a_t) - p_{t \geq k}^{\text{br}}(s_t, a_t)| &= \sum_{s_t, a_t} \left| \frac{1}{k} \sum_{i=0}^{k-1} p_{\pi_{\mathcal{D}}}(s_t, a_t) - \frac{1}{k} \sum_{i=0}^{k-1} p_{t \geq k, i}^{\text{br}}(s_t, a_t) \right| \\
&\leq \frac{1}{k} \sum_{i=0}^{k-1} \sum_{s_t, a_t} |p_\pi(s_t, a_t) - p_{t \geq k, i}^{\text{br}}(s_t, a_t)| \\
&\leq \frac{1}{k} \sum_{i=0}^{k-1} \{(k-i)2\epsilon_{m'} + (t-k+i)2\epsilon_\pi\} \\
&= \frac{1}{k} \{2k^2\epsilon_{m'} - (k-1)k\epsilon_{m'} + 2tk\epsilon_\pi - 2k^2\epsilon_\pi + (k-1)k\epsilon_\pi\} \\
&= \frac{1}{k} \{2kt\epsilon_\pi + 2(\epsilon_{m'} - \epsilon_\pi)k^2 - (k-1)k(\epsilon_{m'} - \epsilon_\pi)\} \\
&= \frac{1}{k} \{2kt\epsilon_\pi + (\epsilon_{m'} - \epsilon_\pi)k^2 + k(\epsilon_{m'} - \epsilon_\pi)\} \tag{29}
\end{aligned}$$

By substituting Eqs. 19, 28, and 29, into Eq. 18, we obtain the result:

$$\begin{aligned}
|\mathbb{E}_{\pi, p}[R] - \mathbb{E}_{\mathcal{D}_{\text{model}}}[R]| &\leq r_{\max} \left\{ \frac{2\epsilon_\pi + \sum_{t=1}^{k-1} \gamma^t \{t(\epsilon_{m'} + \epsilon_\pi) + (\epsilon_{m'} - \epsilon_\pi)\}}{\sum_{t=k}^{\infty} \gamma^t \left\{ \frac{1}{k} \{2kt\epsilon_\pi + (\epsilon_{m'} - \epsilon_\pi)k^2 + k(\epsilon_{m'} - \epsilon_\pi)\} \right\}} \right\} \\
&= r_{\max} \left\{ \frac{2\epsilon_\pi + \frac{1-k\gamma^{(k-1)} + (k-1)\gamma^k}{(1-\gamma)^2} \gamma(\epsilon_{m'} + \epsilon_\pi) + \frac{\gamma^k - \gamma}{\gamma - 1} (\epsilon_{m'} - \epsilon_\pi)}{\sum_{t=k}^{\infty} \gamma^t \frac{1}{k} \{2kt\epsilon_\pi + (\epsilon_{m'} - \epsilon_\pi)k^2 + k(\epsilon_{m'} - \epsilon_\pi)\}} \right\} \\
&= r_{\max} \left\{ \frac{2\epsilon_\pi + \frac{1-k\gamma^{(k-1)} + (k-1)\gamma^k}{(1-\gamma)^2} \gamma(\epsilon_{m'} + \epsilon_\pi) + \frac{\gamma^k - \gamma}{\gamma - 1} (\epsilon_{m'} - \epsilon_\pi)}{\sum_{t=1}^{\infty} \gamma^t \frac{1}{k} \{2kt\epsilon_\pi + (\epsilon_{m'} - \epsilon_\pi)k^2 + k(\epsilon_{m'} - \epsilon_\pi)\} - \sum_{t=1}^{k-1} \gamma^t \frac{1}{k} \{2kt\epsilon_\pi + (\epsilon_{m'} - \epsilon_\pi)k^2 + k(\epsilon_{m'} - \epsilon_\pi)\}} \right\} \\
&= r_{\max} \left\{ \frac{2\epsilon_\pi + \frac{1-k\gamma^{(k-1)} + (k-1)\gamma^k}{(1-\gamma)^2} \gamma(\epsilon_{m'} + \epsilon_\pi) + \frac{\gamma^k - \gamma}{\gamma - 1} (\epsilon_{m'} - \epsilon_\pi)}{\frac{1}{(1-\gamma)^2} 2\gamma\epsilon_\pi + \frac{\gamma}{1-\gamma} \{(\epsilon_{m'} - \epsilon_\pi)k + (\epsilon_{m'} - \epsilon_\pi)\} - \frac{1-k\gamma^{(k-1)} + (k-1)\gamma^k}{(1-\gamma)^2} 2\gamma\epsilon_\pi - \frac{\gamma^k - \gamma}{\gamma - 1} \{(\epsilon_{m'} - \epsilon_\pi)k + (\epsilon_{m'} - \epsilon_\pi)\}} \right\} \\
&= r_{\max} \left\{ \frac{\frac{1+\gamma^2}{(1-\gamma)^2} 2\epsilon_\pi + \frac{\gamma - k\gamma^k + (k-1)\gamma^{k+1}}{(1-\gamma)^2} (\epsilon_{m'} - \epsilon_\pi)}{\frac{\gamma^k - \gamma}{\gamma - 1} (\epsilon_{m'} - \epsilon_\pi) + \left(\frac{\gamma}{1-\gamma} - \frac{\gamma^k - \gamma}{\gamma - 1} \right) (k+1)(\epsilon_{m'} - \epsilon_\pi)} \right\} \\
&= r_{\max} \left\{ \frac{\frac{1+\gamma^2}{(1-\gamma)^2} 2\epsilon_\pi + \frac{\gamma - k\gamma^k + (k-1)\gamma^{k+1}}{(1-\gamma)^2} (\epsilon_{m'} - \epsilon_\pi)}{\frac{\gamma^k - \gamma}{\gamma - 1} (\epsilon_{m'} - \epsilon_\pi) + \frac{\gamma^k}{1-\gamma} (k+1)(\epsilon_{m'} - \epsilon_\pi)} \right\} \tag{30}
\end{aligned}$$

□

A.6 The relation of returns in the case where a reward prediction is inaccurate

In Section 5, we discuss the relation between the true returns and the returns estimated on the meta-model under the assumption that the reward prediction error is zero. The theoretical result under this assumption is still useful because there are many cases where the true reward function is given and the reward prediction is not required. However, a number of readers still may want to know what the relation of the returns is under the assumption that the reward prediction is inaccurate. In this section, we provide the relation of the returns under inaccurate reward prediction in the MDP case¹⁴.

We start our discussion by defining the bound of the reward prediction error ϵ_r :

¹⁴Here, we do not discuss the theorems in the POMDP case because those in the MDP case can be easily extended into the POMDP case by utilizing Lemma 1.

Definition 3. $\epsilon_r := \max_t \mathbb{E}_{(a_t, s_t) \sim \mathcal{D}_{\text{model}}} [|r(s_t, a_t) - r_\theta(s_t, a_t)|]$, where $r_\theta(s_t, a_t) := \mathbb{E}_{r_t \sim p_\theta} [r_t | a_t, s_t]$.

We also define the return on the branched rollout with inaccurate reward prediction.

$$\begin{aligned} \mathbb{E}_{\mathcal{D}_{\text{model}}} [\hat{R}] &:= \sum_{s_0, a_0} p_{\pi_{\mathcal{D}}} (s_0, a_0) r_\theta(s_0, a_0) + \sum_{t=1}^{k-1} \sum_{s_t, a_t} \gamma^t p_{t < k}^{\text{br}}(s_t, a_t) r_\theta(s_t, a_t) \\ &\quad + \sum_{t=k}^{\infty} \sum_{s_t, a_t} \gamma^t p_{t \geq k}^{\text{br}}(s_t, a_t) r_\theta(s_t, a_t) \end{aligned} \quad (31)$$

Now, we provide the relation between the returns under inaccurate reward prediction.

Theorem 6 (Extension of Theorem 4 into the case where reward prediction is inaccurate). *Under the k -branched rollout, using the bound of a model error under $\pi_{\mathcal{D}}$, $\epsilon_m = \max_t \mathbb{E}_{a \sim \pi_{\mathcal{D}}, s \sim p, t} [D_{TV}(p(s'|s, a) || p_\theta(s'|s, a))]$, the bound of the policy shift $\epsilon_\pi = \max_s D_{TV}(\pi || \pi_{\mathcal{D}})$ and the bound of the reward prediction error $\epsilon_r = \max_t \mathbb{E}_{(a_t, s_t) \sim \mathcal{D}_{\text{model}}} [|r(s_t, a_t) - r_\theta(s_t, a_t)|]$, the following inequation holds,*

$$\begin{aligned} \mathbb{E}_{\pi, p} [R] &\geq \mathbb{E}_{\mathcal{D}_{\text{model}}} [\hat{R}] - r_{\max} \left\{ \frac{1 + \gamma^2}{(1 - \gamma)^2} 2\epsilon_\pi + \frac{\gamma - k\gamma^k + (k-1)\gamma^{k+1}}{(1 - \gamma)^2} (\epsilon_\pi + \epsilon_m) \right. \\ &\quad \left. + \frac{\gamma^k - \gamma}{\gamma - 1} (\epsilon_\pi + \epsilon_m) + \frac{\gamma^k}{1 - \gamma} (k+1)(\epsilon_\pi + \epsilon_m) \right\} - \frac{\gamma}{1 - \gamma} \epsilon_r. \end{aligned} \quad (32)$$

Proof.

$$\begin{aligned} \left| \mathbb{E}_{\pi, p} [R] - \mathbb{E}_{\mathcal{D}_{\text{model}}} [\hat{R}] \right| &= \left| \mathbb{E}_{\pi, p} [R] - \mathbb{E}_{\mathcal{D}_{\text{model}}} [R] + \mathbb{E}_{\mathcal{D}_{\text{model}}} [R] - \mathbb{E}_{\mathcal{D}_{\text{model}}} [\hat{R}] \right| \\ &\leq \left| \mathbb{E}_{\pi, p} [R] - \mathbb{E}_{\mathcal{D}_{\text{model}}} [R] \right| + \left| \mathbb{E}_{\mathcal{D}_{\text{model}}} [R] - \mathbb{E}_{\mathcal{D}_{\text{model}}} [\hat{R}] \right| \end{aligned} \quad (33)$$

$$\begin{aligned} \left| \mathbb{E}_{\mathcal{D}_{\text{model}}} [R] - \mathbb{E}_{\mathcal{D}_{\text{model}}} [\hat{R}] \right| &= \left| \sum_{s_0, a_0} p_{\pi_{\mathcal{D}}} (s_0, a_0) \{r(s_0, a_0) - r_\theta(s_0, a_0)\} \right. \\ &\quad \left. + \sum_{t=1}^{k-1} \sum_{s_t, a_t} \gamma^t p_{t < k}^{\text{br}}(s_t, a_t) \{r(s_t, a_t) - r_\theta(s_t, a_t)\} \right. \\ &\quad \left. + \sum_{t=k}^{\infty} \sum_{s_t, a_t} \gamma^t p_{t \geq k}^{\text{br}}(s_t, a_t) \{r(s_t, a_t) - r_\theta(s_t, a_t)\} \right| \\ &\leq \sum_{s_0, a_0} p_{\pi_{\mathcal{D}}} (s_0, a_0) |r(s_0, a_0) - r_\theta(s_0, a_0)| \\ &\quad + \sum_{t=1}^{k-1} \sum_{s_t, a_t} \gamma^t p_{t < k}^{\text{br}}(s_t, a_t) |r(s_t, a_t) - r_\theta(s_t, a_t)| \\ &\quad + \sum_{t=k}^{\infty} \sum_{s_t, a_t} \gamma^t p_{t \geq k}^{\text{br}}(s_t, a_t) |r(s_t, a_t) - r_\theta(s_t, a_t)| \\ &\leq \sum_{t=0}^{\infty} \gamma^t \epsilon_r \\ &= \frac{\gamma}{1 - \gamma} \epsilon_r \end{aligned} \quad (34)$$

By substituting Eqs. 26 and 34 into Eq. 33, we obtain the result:

$$\left| \mathbb{E}_{\pi, p} [R] - \mathbb{E}_{\mathcal{D}_{\text{model}}} [\hat{R}] \right| \leq r_{\max} \left\{ \frac{1 + \gamma^2}{(1 - \gamma)^2} 2\epsilon_\pi + \frac{\gamma - k\gamma^k + (k-1)\gamma^{k+1}}{(1 - \gamma)^2} (\epsilon_\pi + \epsilon_m) \right\} + \frac{\gamma}{1 - \gamma} \epsilon_r \quad (35)$$

□

Theorem 7 (Extension of Theorem 5 into the case where reward prediction is inaccurate). Let $\epsilon_{m'} \geq \max_t E_{a \sim \pi, s \sim p} [D_{TV}(p(s'|s, a) || p_\theta(s'|s, a))]$ and $\epsilon_r = \max_t \mathbb{E}_{(a_t, s_t) \sim \mathcal{D}_{model}} [|r(s_t, a_t) - r_\theta(s_t, a_t)|]$,

$$\begin{aligned} \mathbb{E}_{\pi, p} [R] \geq \mathbb{E}_{\mathcal{D}_{model}} [\hat{R}] - r_{max} \left\{ \frac{1 + \gamma^2}{(1 - \gamma)^2} 2\epsilon_\pi + \frac{\gamma - k\gamma^k + (k - 1)\gamma^{k+1}}{(1 - \gamma)^2} (\epsilon_\pi - \epsilon_{m'}) \right. \\ \left. + \frac{\gamma^k - \gamma}{\gamma - 1} (\epsilon_\pi - \epsilon_{m'}) + \frac{\gamma^k}{1 - \gamma} (k + 1) (\epsilon_\pi - \epsilon_{m'}) \right\} - \frac{\gamma}{1 - \gamma} \epsilon_r. \end{aligned} \quad (36)$$

Proof. Similar to the derivation of Theorem 6, we obtain the result by substituting Eq. 30 and 34 into Eq. 33. \square

A.7 PEARL in Sections 6 and 7

The PEARL algorithm used in Sections 6 and 7 refers to “PEARL with RNN-traj” in [26]. Although PEARL with RNN-traj performed worse than vanilla PEARL and its variant (PEARL with RNN-tran) in the original paper [26], we found that PEARL RNN-traj works best in our setup, and thus decided to use it for our implementation of M3PO and experiments.

A.8 Baseline methods for our experiment

PEARL: The model-free meta-RL method proposed in [26]. This is an off-policy method and implemented by extending Soft Actor-Critic [11]. By leveraging experience replay, this method shows high sample efficiency. We reimplemented the PEARL on TensorFlow, referring to the original implementation on PyTorch (<https://github.com/katerakelly/oyster>).

Learning to adapt (L2A): The meta-model-based RL proposed in [22]. In this method, the meta-model is implemented with MAML [7] and the optimal action is found by the model predictive path integral control [38] on the full meta-model based rollouts. We adapt the following implementation of L2A to our experiment: https://github.com/iclavera/learning_to_adapt

A.9 Environments for our experiment

For our experiment in Section 7, we prepare simulated robot environments using the MuJoCo physics engine [36] (Figure 5):

Halfcheetah-fwd-bwd: In this environment, meta-policies are used to control the half-cheetah, which is a planar biped robot with eight rigid links, including two legs and a torso, along with six actuated joints. Here, the half-cheetah’s moving direction is randomly selected from “forward” and “backward” around every 15 seconds (in simulation time). If the half-cheetah moves in the correct direction, a positive reward is fed to the half-cheetah in accordance with the magnitude of movement, otherwise, a negative reward is fed.

Halfcheetah-pier: In this environment, the half-cheetah runs over a series of blocks that are floating on water. Each block moves up and down when stepped on, and the changes in the dynamics are rapidly changing due to each block having different damping and friction properties. These properties are randomly determined at the beginning of each episode.

Ant-fwd-bwd: Same as Halfcheetah-fwd-bwd except that the meta-policies are used for controlling the ant, which is a quadruped robot with nine rigid links, including four legs and a torso, along with eight actuated joints.

Ant-crippled-leg: In this environment, we randomly sample a leg on the ant to cripple. The crippling of the leg causes unexpected and drastic changes to the underlying dynamics. One of the four legs is randomly crippled every 15 seconds.

Walker2D-randomparams: In this environment, the meta-policies are used to control the walker, which is a planar biped robot consisting of seven links, including two legs and a torso, along with six actuated joints. The walker’s torso mass and ground friction is randomly determined every 15 seconds.

Humanoid-direc: In this environment, the meta-policies are used to control the humanoid, which is a biped robot with 13 rigid links, including two legs, two arms and a torso, along with 17 actuated joints. In this task, the humanoid moving direction is randomly selected from two different directions around every 15 seconds. If the humanoid moves in the correct direction, a positive reward

is fed to the humanoid in accordance with the magnitude of its movement, otherwise, a negative reward is fed.

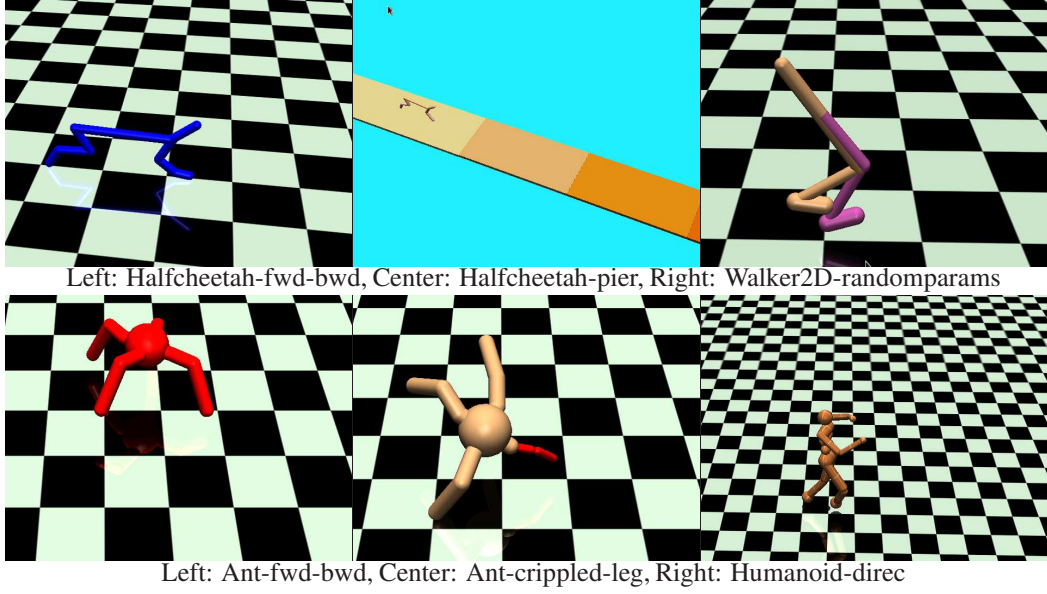


Figure 5: Environments for our experiment

A.10 Complementary experimental results

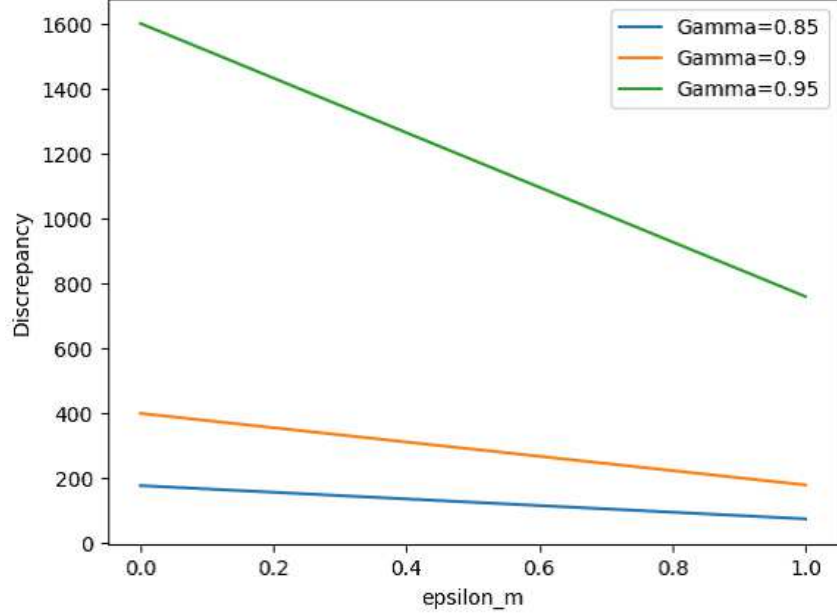


Figure 6: Discrepancy between $\mathbb{E}_{\pi_{\phi}, p}[R]$ and $\mathbb{E}_{\pi_{\phi}, p_{\theta}}[R]$ in Theorem 1. The vertical and horizontal axes represent the discrepancy value and $\epsilon_m \in [0, 1]$, respectively. We set the other variables as $\epsilon_{\pi} = 1 - \epsilon_m$ and $r_{\max} = 1$.

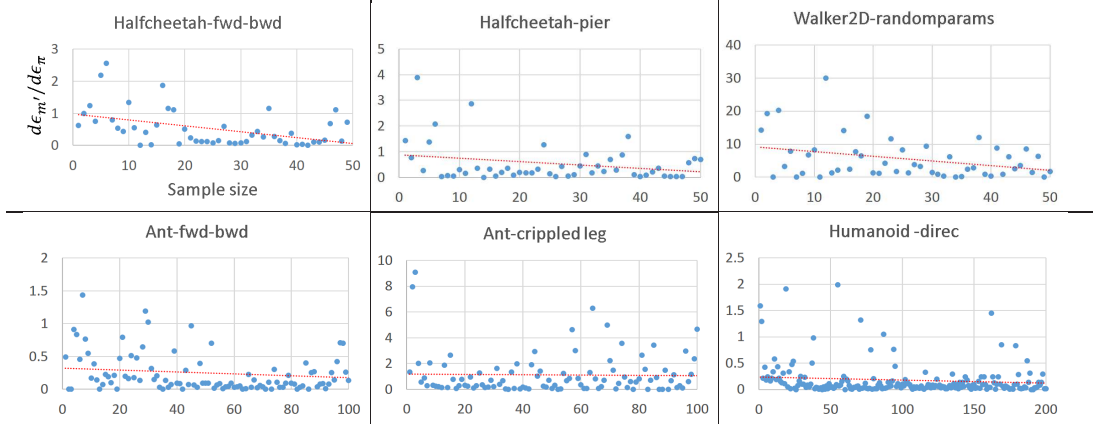


Figure 7: The local change in $\epsilon_{m'}$ with respect to ϵ_{π} versus training sample size. In each figure, the vertical axis represents the local change of the meta-model error ($\frac{d\epsilon_{m'}}{d\epsilon_{\pi}}$) and the horizontal axis represents the training sample size (x1000). The red-dotted line is the linear interpolation of the blue dots, which shows the trend of the local change decreasing as the training sample size grows.

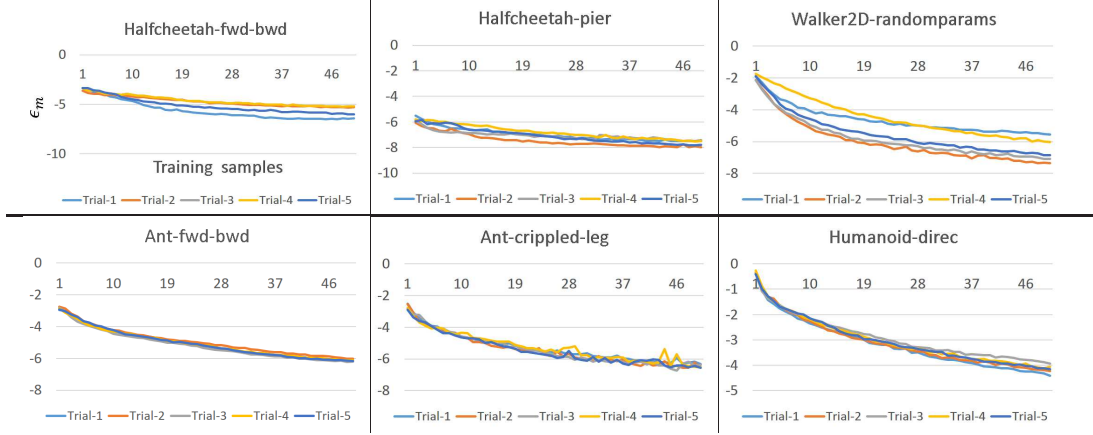


Figure 8: Transition of model errors on training. In each figure, the vertical axis represents empirical values of ϵ_m and the horizontal axis represents the number of training samples (x1000). We ran five trials with different random seeds. The result of the x -th trial is denoted by Trial- x . We used the negative of log-likelihood of the meta-model on validation samples as the approximation of ϵ_m .

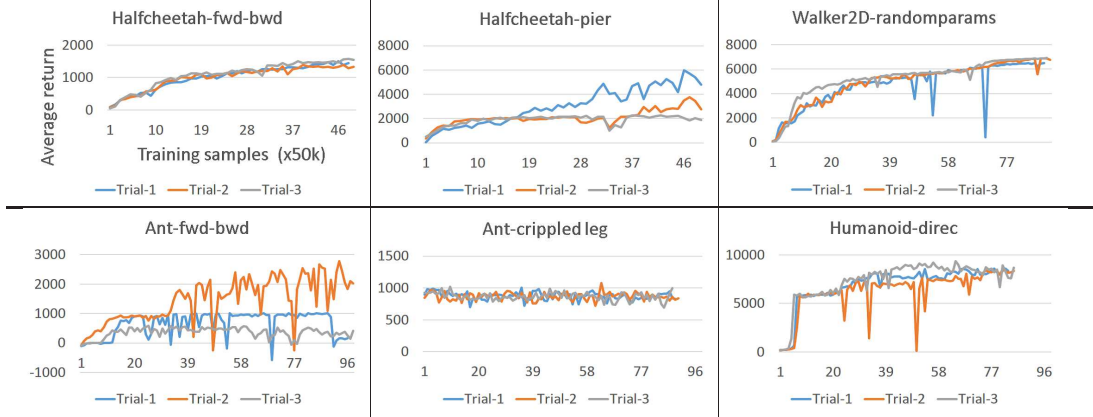


Figure 9: Learning curve of PEARL in a long-term training. In each figure, the vertical axis represents expected returns and the horizontal axis represents the number of training samples (x50000). The meta-policy and meta-model were fixed and their expected returns were evaluated on 50 episodes at every 50,000 training samples. Each method was evaluated in three trials, and the result of the x -th trial is denoted by Trial- x . **Note that the scale of the horizontal axis is larger than that in Figure 2 by 50 times (i.e., 4 in this figure is equal to 200 in Figure 2).**

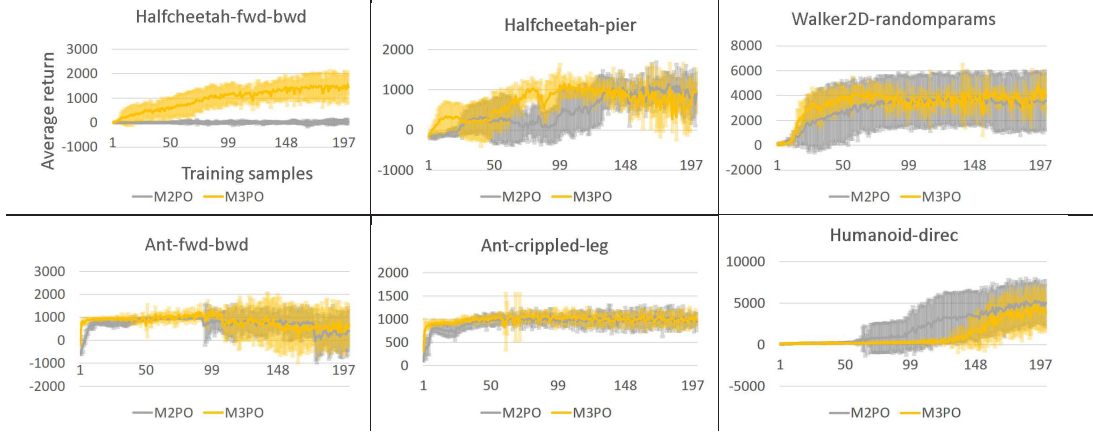


Figure 10: Learning curve of M3PO and M2PO. In each figure, the vertical axis represents expected returns and the horizontal axis represents the number of training samples (x1000). The meta-policy and meta-model (and a predictive model) were fixed and their expected returns were evaluated on 50 episodes at every 1000 training samples for the other methods. In each episode, the task was initialized and changed randomly. Each method was evaluated in at least five trials, and the expected return on the 50 episodes was further averaged over the trials. The averaged expected returns and their standard deviations are plotted in the figures.

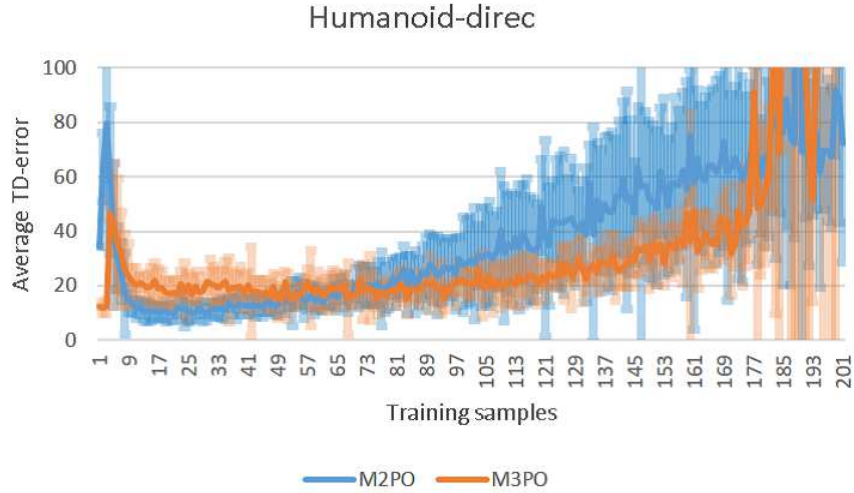


Figure 11: Transition of TD-errors (Q-function error) on training. In each figure, the vertical axis represents empirical values of ϵ_m and the horizontal axis represents the number of training samples (x1000). We ran ten trials with different random seeds and plotted the average of their results. The error bar means one standard deviation.

A.11 Complementary analysis

In addition to Q1 and Q2 in the main content, we also conducted a complementary analysis to answer the following question. **Q.3:** Does the use of a meta-model in M3PO contribute to the improvement of the meta-policy?

In an analysis in this section, we compare M3PO with the following method. **Model-based Meta-Policy Optimization (M2PO):** This method is a variant of M3PO, in which a non-adaptive predictive model is used instead of the meta-model. The predictive model architecture is the same as that in the MBPO algorithm [15] (i.e., the ensemble of Gaussian distributions based on four-layer feed-forward neural networks).

Regarding Q3, our experimental result indicates that the use of a meta-model contributed to the performance improvement in a number of the environments. In Figure 10 in the appendix, we can clearly see the improvement of M3PO against M2PO in Halfcheetah-fwd-bwd. In addition, in the Ant environments, although the M3PO’s performance is seemingly the same as that of M2PO, the qualitative performance is quite different; the M3PO can produce the meta-policy for walking in the correct direction, while M2PO failed to do so (M2PO produces the meta-policy “always standing” with a very small amount of control signal). For Humanoid-direc, in contrast, M2PO tends to achieve a better sample efficiency than M3PO. We hypothesize that the primary reason for this is that during the plateau at the early stage of training in Humanoid-direc, the predictive model used in M2PO generates fictitious trajectories that make meta-policy optimization more stable. To verify this hypothesis, we compare TD-errors (Q-function errors) during training, which is an indicator of the stability of meta-policy optimization, in M3PO and M2PO. The evaluation result (Figure 11 in the appendix) shows that during the performance plateau (10–60 epoch), the TD-error in M2PO was actually lower than that in M3PO; this result supports our hypothesis. In this paper, we did not focus on the study of meta-model usage to generate the trajectories that make meta-policy optimization stable, but this experimental result indicates that such a study is important for further improving M3PO.

A.12 Hyperparameter setting

Table 1: Hyperparameter settings for M3PO results shown in Figure 2. $x \rightarrow y$ over epochs $a \rightarrow b$ denotes a thresholded linear function, i.e., at epoch e , $f(e) = \min(\max(x + \frac{e-a}{b-a} \cdot (y-x), x), y)$

		Halfcheetah-fwd-bwd	Halfcheetah-pier	Ant-fwd-bwd	Ant-crippled-leg	Walker2D-randomparams	Humanoid-direc
N	epoch	200					
E	environment step per epoch	1000					
M	meta-model rollouts per epoch	1e6			5e5	1e6	
B	ensemble size	3					
G	meta-policy update per environment step	40		20			
k	meta-model horizon	1	1	1 \rightarrow 25 over epoch 20 \rightarrow 100		1	1